fractal and fractional

Article

Jacobi Spectral Collocation Technique for Time-Fractional Inverse Heat Equations

Mohamed A. Abdelkawy [1,2,*], Ahmed Z. M. Amin [3], Mohammed M. Babatin [1], Abeer S. Alnahdi [1], Mahmoud A. Zaky [4] and Ramy M. Hafez [5]

[1] Department of Mathematics and Statistics, College of Science, Imam Mohammad Ibn Saud Islamic University, Riyadh 13318, Saudi Arabia; mmbabatin@imamu.edu.sa (M.M.B.); ASAlnahdi@imamu.edu.sa (A.S.A.)
[2] Department of Mathematics, Faculty of Science, Beni-Suef University, Beni-Suef 65211, Egypt
[3] Department of Mathematical Sciences, Faculty of Science, Technology, Universiti Kebangsaan Malaysia (UKM), Bangi 43600, Malaysia; P108214@siswa.ukm.edu.my
[4] Department of Applied Mathematics, National Research Centre, Cairo 12622, Egypt; ma.zaky@yahoo.com
[5] Faculty of Education, Matrouh University, Matrouh 51512, Egypt; r_mhafez@yahoo.com
* Correspondence: maohamed@imamu.edu.sa

Abstract: In this paper, we introduce a numerical solution for the time-fractional inverse heat equations. We focus on obtaining the unknown source term along with the unknown temperature function based on an additional condition given in an integral form. The proposed scheme is based on a spectral collocation approach to obtain the two independent variables. Our approach is accurate, efficient, and feasible for the model problem under consideration. The proposed Jacobi spectral collocation method yields an exponential rate of convergence with a relatively small number of degrees of freedom. Finally, a series of numerical examples are provided to demonstrate the efficiency and flexibility of the numerical scheme.

Keywords: inverse problem; spectral collocation method; fractional diffusion; fractional calculus

MSC: 35R30; 65M70; 35R11

Citation: Abdelkawy, M.A.; Amin, A.Z.M.; Babatin, M.M.; Alnahd, A.S.; Zaky, M.A.; Hafez, R.M. Jacobi Spectral Collocation Technique for Time-Fractional Inverse Heat Equations. *Fractal Fract.* **2021**, *5*, 115. https://doi.org/10.3390/fractalfract5030115

Academic Editors: Ivanka Stamova, António M. Lopes and Liping Chen

Received: 8 July 2021
Accepted: 7 September 2021
Published: 9 September 2021

1. Introduction

The concept of fractional derivatives has become one of the key aspects of applied mathematics because it is more suitable for modelling many real-world problems than the local derivative. As a result, the fractional derivative has received considerable attention and development in a wide range of fields [1–5]. Fractional derivatives are defined in a variety of ways in the mathematical literature, including Riemann–Liouville and Caputo fractional derivatives. Hence, fractional differential equations have attracted the attention of researchers in recent years. The main reason for this is that they are commonly used in chemistry [6], mathematical biology systems [7], electrical engineering [8], systems identification, control theory [9], signal processing, mechanical engineering [10–12], finance and fractional dynamics and so on.

Direct fractional-order diffusion equations have been extensively discussed in the literature; see [13–15]. Often, for many practical studies, there is an unknown parameter that is found in the initial or boundary data or the source term that requires an additional measurement. The inverse fractional-order case introduces an appropriate instrument for describing anomalous diffusion phenomena appeared in chemical [16], biological [17,18], hydrological [19], physical [20,21] and engineering [22,23] fields. In contrast to those classical problems, the studies of inverse problems have not satisfactorily been studied. The mathematical problem of studying inverse problems with non-Fourier heat-conduction constitutive models is extremely novel. The goal of inverse problems for heat-conduction process is to set unknown ingredients of the conduction system from some measurement data, which is of major importance in the applied area. Hung and Lin [24] solved the hyperbolic inverse heat-conduction problem. Yang [25] solved the two-dimensional inverse hyperbolic heat problem by modified Newton–Raphson method. Tang and Araki [26] estimated thermal diffusivity and the relaxation parameters for solving the inverse heat equation. Wang and Liu [27] used the total variation regularization method for solving backward time-fractional diffusion problem. Zhang and Xu [28] solved the inverse source problem of the fractional diffusion equation.

Spectral methods are powerful tools for solving different types of differential and integral equations that arise in various fields of science and engineering. In recent decades, they have been adopted in a variety of notable areas [29–38]. In the numerical solutions of fractional differential equations, a variety of spectral methods have recently been used [39,40]. Their major advantages are exponential convergence rates, high accuracy level, and low computational costs. The spectral methods are distinguished over finite difference, finite element, and finite volume in their global, high-accuracy numerical results and have applicability to most problems with integer or fractional orders; see [36,41–43]. Because explicit analytical solutions of space and/or time-fractional differential equations are difficult to obtain in most cases, developing efficient numerical schemes is a very important demand. In various applications, many efficient numerical techniques have been introduced to treat various problems. Presently there is a wide and constantly increasing range of spectral methods and there has been significant growth in fractional differential and integral equations [44] due to their high-order accuracy. Compared to the effort put into analyzing finite difference schemes in the literature for solving fractional-order differential equations, only a little research has been made in developing and analyzing global spectral schemes.

Our main aim in this paper is to provide shifted Jacobi Gauss–Lobatto and shifted Jacobi Gauss–Radau collection schemes for solving fractional inverse heat equations (IHEs). The unknown solution is approximated using the shifted Jacobi polynomials as a truncated series. The collocation technique is provided along with appropriate treatment for addressing the extra condition. This procedure allows us to exclude the unknown function $\mathcal{Q}(\tau)$ from the equation under consideration. As a result, this problem is reduced to a system of algebraic equations by employing the spectral collocation approach. Finally, in terms of shifted Jacobi polynomials, we can extend the unknown functions $\mathcal{U}(\xi,\tau)$ and $\mathcal{Q}(\tau)$. To the best of our knowledge, there are no numerical results on the spectral collocation method for treating the IHEs.

This paper is organized as follows. We introduce some mathematical preliminaries in Section 2. In Section 3.2, we construct the numerical scheme to solve the fractional IHEs with initial-boundary conditions and nonlocal conditions. In Section 4, we solve and analyze some examples to illustrate the efficiency and accuracy of the method. In Section 5, we provide the main conclusions.

2. Preliminaries and Notations

This section introduces some properties of the shifted Jacobi polynomials. The Jacobi polynomials are defined as follows:

$$\begin{aligned}
&\mathcal{G}_{k+1}^{(\sigma_1,\varrho_1)}(y) = (a_k^{(\sigma_1,\varrho_1)} y - b_k^{(\sigma_1,\varrho_1)})\mathcal{G}_k^{(\sigma_1,\varrho_1)}(y) - c_k^{(\sigma_1,\varrho_1)}\mathcal{G}_{k-1}^{(\sigma_1,\varrho_1)}(y), \quad k \geq 1,\\
&\mathcal{G}_0^{(\sigma_1,\varrho_1)}(y) = 1, \quad \mathcal{G}_1^{(\sigma_1,\varrho_1)}(y) = \frac{1}{2}(\sigma_1+\varrho_1+2)y + \frac{1}{2}(\sigma_1-\varrho_1),
\end{aligned}$$

$$\mathcal{G}_k^{(\sigma_1,\varrho_1)}(-y) = (-1)^k \mathcal{G}_k^{(\sigma_1,\varrho_1)}(y), \quad \mathcal{G}_k^{(\sigma_1,\varrho_1)}(-1) = \frac{(-1)^k\Gamma(k+\varrho_1+1)}{k!\Gamma(\varrho_1+1)}, \tag{1}$$

where $\sigma_1,\ \varrho_1 > -1, y \in (-1,1)$ and

$$a_k^{(\sigma_1,\varrho_1)} = \frac{(2k+\sigma_1+\varrho_1+1)(2k+\sigma_1+\varrho_1+2)}{2(k+1)(k+\sigma_1+\varrho_1+1)},$$
$$b_k^{(\sigma_1,\varrho_1)} = \frac{(\varrho_1^2-\sigma_1^2)(2k+\sigma_1+\varrho_1+1)}{2(k+1)(k+\sigma_1+\varrho_1+1)(2k+\sigma_1+\varrho_1)},$$
$$c_k^{(\sigma_1,\varrho_1)} = \frac{(k+\sigma_1)(k+\varrho_1)(2k+\sigma_1+\varrho_1+2)}{(k+1)(k+\sigma_1+\varrho_1+1)(2k+\sigma_1+\varrho_1)}.$$

The nth-order derivative (n is an integer) of $\mathcal{G}_j^{(\sigma_1,\varrho_1)}(y)$ can also be obtained from

$$D^n \mathcal{G}_j^{(\sigma_1,\varrho_1)}(y) = \frac{\Gamma(j+\sigma_1+\varrho_1+q+1)}{2^n\Gamma(j+\sigma_1+\varrho_1+1)}\mathcal{G}_{j-n}^{(\sigma_1+n,\varrho_1+n)}(y). \tag{2}$$

The analytic form of the shifted Jacobi polynomial $\mathcal{G}_{L,k}^{(\sigma_1,\varrho_1)}(y) = \mathcal{G}_k^{(\sigma_1,\varrho_1)}(\frac{2y}{L}-1),\ L>0,$ is written as

$$\begin{aligned}\mathcal{G}_{L,k}^{(\sigma_1,\varrho_1)}(y) &= \sum_{j=0}^{k}(-1)^{k-j}\frac{\Gamma(k+\varrho_1+1)\Gamma(j+k+\sigma_1+\varrho_1+1)}{\Gamma(j+\varrho_1+1)\Gamma(k+\sigma_1+\varrho_1+1)(k-j)!j!L^j}y^j \\ &= \sum_{j=0}^{k}\frac{\Gamma(k+\sigma_1+1)\Gamma(k+j+\sigma_1+\varrho_1+1)}{j!(k-j)!\Gamma(j+\sigma_1+1)\Gamma(k+\sigma_1+\varrho_1+1)L^j}(y-L)^j.\end{aligned} \tag{3}$$

As a result, for any integer n, we can derive the following properties

$$\begin{aligned}\mathcal{G}_{L,k}^{(\sigma_1,\varrho_1)}(0) &= (-1)^k\frac{\Gamma(k+\varrho_1+1)}{\Gamma(\varrho_1+1)\,k!}, \\ \mathcal{G}_{L,k}^{(\sigma_1,\varrho_1)}(L) &= \frac{\Gamma(k+\sigma_1+1)}{\Gamma(\sigma_1+1)\,k!},\end{aligned} \tag{4}$$

$$D^n\mathcal{G}_{L,k}^{(\sigma_1,\varrho_1)}(0) = \frac{(-1)^{k-n}\Gamma(k+\varrho_1+1)(k+\sigma_1+\varrho_1+1)_n}{L^n\Gamma(k-n+1)\Gamma(n+\varrho_1+1)}, \tag{5}$$

$$D^n\mathcal{G}_{L,k}^{(\sigma_1,\varrho_1)}(L) = \frac{\Gamma(k+\sigma_1+1)(k+\sigma_1+\varrho_1+1)_n}{L^n\Gamma(k-n+1)\Gamma(n+\sigma_1+1)}, \tag{6}$$

$$D^n\mathcal{G}_{L,k}^{(\sigma_1,\varrho_1)}(y) = \frac{\Gamma(n+k+\sigma_1+\varrho_1+1)}{L^n\Gamma(k+\sigma_1+\varrho_1+1)}\mathcal{G}_{L,k-n}^{(\sigma_1+n,\varrho_1+n)}(y). \tag{7}$$

Let $w_L^{(\sigma_1,\varrho_1)}(y) = (L-y)^{\sigma_1}y^{\varrho_1}$. Then, we define

$$(u,v)_{w_L^{(\sigma_1,\varrho_1)}} = \int_0^L u(y)\,v(y)\,w_L^{(\sigma_1,\varrho_1)}(y)\,dy, \quad \|v\|_{w_L^{(\sigma_1,\varrho_1)}} = (v,v)^{\frac{1}{2}}_{w_L^{(\sigma_1,\varrho_1)}}. \tag{8}$$

The set of the shifted Jacobi polynomials forms a complete $L^2_{w_L^{(\sigma_1,\varrho_1)}}[0,L]$-orthogonal system. Furthermore, and as a result of (8), we have

$$\|\mathcal{G}_{L,k}^{(\sigma_1,\varrho_1)}\|^2_{w_L^{(\sigma_1,\varrho_1)}} = \left(\frac{L}{2}\right)^{\sigma_1+\varrho_1+1} h_k^{(\sigma_1,\varrho_1)} = h_{L,k}^{(\sigma_1,\varrho_1)}, \tag{9}$$

where

$$h_n^{(\sigma_1,\varrho_1)} = \frac{2^{\sigma_1+\varrho_1+1}\Gamma(n+\varrho_1+1)\Gamma(n+\sigma_1+1)}{n!\Gamma(n+\sigma_1+\varrho_1+1)(2n+\sigma_1+\varrho_1+1)}.$$

We denote $y_{N,j}^{(\sigma_1,\varrho_1)}$ and $\varpi_{N,j}^{(\sigma_1,\varrho_1)}$, $0 \leq j \leq N$, the nodes and Christoffel numbers on the interval $[-1,1]$. For the shifted Jacobi on the interval $[0,L]$, we obtain

$$y_{L,N,j}^{(\sigma_1,\varrho_1)} = \frac{L}{2}(y_{N,j}^{(\sigma_1,\varrho_1)} + 1),$$

$$\varpi_{L,N,j}^{(\sigma_1,\varrho_1)} = (\frac{L}{2})^{\sigma_1+\varrho_1+1}\varpi_{N,j}^{(\sigma_1,\varrho_1)},\ 0 \leq j \leq N.$$

Applying the quadrature rule, for $\phi \in S_{2N+1}[0,L]$, we obtain

$$\begin{aligned}\int_0^L (L-y)^{\sigma_1} y^{\varrho_1}\phi(y)dy &= \left(\frac{L}{2}\right)^{\sigma_1+\varrho_1+1}\int_{-1}^1 (1-y)^{\sigma_1}(1+y)^{\varrho_1}\phi\left(\frac{L}{2}(y+1)\right)dy \\ &= \left(\frac{L}{2}\right)^{\sigma_1+\varrho_1+1}\sum_{j=0}^N \varpi_{N,j}^{(\sigma_1,\varrho_1)}\phi\left(\frac{L}{2}(y_{N,j}^{(\sigma_1,\varrho_1)}+1)\right) \\ &= \sum_{j=0}^N \varpi_{L,N,j}^{(\sigma_1,\varrho_1)}\phi\left(y_{L,N,j}^{(\sigma_1,\varrho_1)}\right),\end{aligned} \tag{10}$$

where $S_N[0,L]$ is the set of polynomials of degree at most N.

3. Fully Spectral Collocation Treatment

3.1. Initial-Boundary Conditions

First, we developed a numerical technique for dealing with the time-fractional IHEs of the form:

$$\frac{\partial^\nu}{\partial\tau^\nu}\Big(\mathcal{U}(\xi,\tau) - \mathcal{U}(\xi,0)\Big) = \frac{\partial^2}{\partial\xi^2}(\mathcal{U}(\xi,\tau)) + \mathcal{Q}(\tau)\Delta(\xi,\tau), \quad (\xi,\tau) \in \Lambda^\bullet \times \Lambda^\diamond, \tag{11}$$

$$\begin{aligned}\mathcal{U}(\xi,0) &= \lambda_1(\xi), \quad \xi \in \Lambda^\bullet, \\ \mathcal{U}(0,\tau) &= \lambda_2(\tau), \quad \mathcal{U}(\xi_{end},\tau) = \lambda_3(\tau), \quad \tau \in \Lambda^\diamond,\end{aligned} \tag{12}$$

where ξ and τ are used for spatial and temporal variables, respectively. The fractional derivative term $\frac{\partial^\nu}{\partial\tau^\nu}\Big(\mathcal{U}(\xi,\tau) - \mathcal{U}(\xi,0)\Big)$ instead of $\frac{\partial^\nu}{\partial\tau^\nu}\Big(\mathcal{U}(\xi,\tau)$ is not only to eschew the singularity at zero, but also provide a significative initial condition, where fractional integral is not included [45].

Where $\frac{\partial^\nu}{\partial\tau^\nu}$ is the fractional temporal derivative in Riemann–Liouville sense,

$$\frac{\partial^\nu \mathcal{U}(\xi,\tau)}{\partial\tau^\nu} = \frac{1}{\Gamma(1-\nu)}\frac{\partial}{\partial\tau}\int_0^\tau \frac{\mathcal{U}(\xi,s)}{(s-\tau)^\mu}ds,$$

and $\Lambda^\bullet \equiv [0,\xi_{end}]$, $\Lambda^\diamond \equiv [0,\tau_{end}]$, $\mathcal{U}(\xi,\tau)$ and $\mathcal{Q}(\tau)$ are unknown functions, while $\Delta(\xi,\tau)$ is a given function. The complexity of the suggested problem is that the function $\mathcal{Q}(\tau)$ is unknown, which necessitates the determination of an additional condition. To resolve this problem, we use the following energy condition

$$\int_0^1 \mathcal{U}(\xi,\tau)d\xi = \mathcal{E}(\tau). \tag{13}$$

Here, the shifted Jacobi Gauss–Lobatto collection method and the shifted Jacobi Gauss–Radau collection scheme are applied to convert the IHEs into a linear system of algebraic equations. We approximate the solution as,

$$\mathcal{U}_{\mathcal{N},\mathcal{M}}(\xi,\tau) = \sum_{\substack{r_1=0,\ldots,\mathcal{N} \\ r_2=0,\ldots,\mathcal{M}}} \varsigma_{r_1,r_2} \mathcal{G}^{\sigma_1,\varrho_1}_{\xi_{end},r_1}(\xi) \mathcal{G}^{\sigma_2,\varrho_2}_{\tau_{end},r_2}(\tau), \tag{14}$$

where $\mathcal{G}^{\sigma,\varsigma}_{\xi_{end},s}(\zeta)$ is used for shifted Jacobi polynomials on $[0,\xi_{end}]$.

The first derivative $\frac{\partial}{\partial x}(\mathcal{U}_{\mathcal{N},\mathcal{M}}(\xi,\tau))$ is given as

$$\frac{\partial}{\partial \xi}(\mathcal{U}_{\mathcal{N},\mathcal{M}}(\xi,\tau)) = \sum_{\substack{r_1=0,\ldots,\mathcal{N} \\ r_2=0,\ldots,\mathcal{M}}} \varsigma_{r_1,r_2} \widetilde{\mathcal{G}}^{\sigma_1,\varrho_1}_{\xi_{end},r_1}(\xi) \mathcal{G}^{\sigma_2,\varrho_2}_{\tau_{end},r_2}(\tau), \tag{15}$$

where $\widetilde{\mathcal{G}}^{\sigma_1,\varrho_1}_{\xi_{end},r_1}(\xi) = \frac{\partial}{\partial x}(\mathcal{G}^{\sigma_1,\varrho_1}_{\xi_{end},r_1}(\xi))$. Similarly, we find

$$\frac{\partial^2}{\partial x^2}(\mathcal{U}_{\mathcal{N},\mathcal{M}}(\xi,\tau)) = \sum_{\substack{r_1=0,\ldots,\mathcal{N} \\ r_2=0,\ldots,\mathcal{M}}} \varsigma_{r_1,r_2} \widehat{\mathcal{G}}^{\sigma_1,\varrho_1}_{\xi_{end},r_1}(\xi) \mathcal{G}^{\sigma_2,\varrho_2}_{\tau_{end},r_2}(\tau), \tag{16}$$

where $\widehat{\mathcal{G}}^{\sigma_1,\varrho_1}_{\xi_{end},r_1}(\zeta) = \frac{\partial^2}{\partial \xi^2}(\mathcal{G}^{\sigma_1,\varrho_1}_{\xi_{end},r_1}(\xi))$. Please note that $\frac{\partial}{\partial \xi}(\mathcal{G}^{\sigma_1,\varrho_1}_{\xi_{end},r_1}(\xi))$ and $\frac{\partial^2}{\partial \xi^2}(\mathcal{G}^{\sigma_1,\varrho_1}_{\xi_{end},r_1}(\xi))$ can be directly computed using (7). However, the fractional temporal derivative in Riemann–Liouville sense is computed as

$$\frac{\partial^\nu}{\partial t^\nu}(\mathcal{U}(\xi,\tau)) = \sum_{\substack{r_1=0,\ldots,\mathcal{N} \\ r_2=0,\ldots,\mathcal{M}}} \varsigma_{r_1,r_2} \mathcal{G}^{\sigma_1,\varrho_1}_{\xi_{end},r_1}(\xi) \tilde{\mathcal{G}}^{\sigma_2,\varrho_2}_{\tau_{end},r_2}(\tau), \tag{17}$$

where $\tilde{\mathcal{G}}^{\sigma_2,\varrho_2}_{\tau_{end},r_2}(\tau) = \frac{\partial^\nu}{\partial \tau^\nu}(\mathcal{G}^{\sigma_2,\varrho_2}_{\tau_{end},r_2}(\tau))$. Using (3), we obtain

$$\begin{aligned} \frac{\partial^\nu}{\partial \tau^\nu}(\mathcal{G}^{\sigma_2,\varrho_2}_{\tau_{end},r_2}(\tau)) &= \sum_{k=0}^{r_2} (-1)^{r_2-k} \frac{\Gamma(r_2+\varrho_2+1)\Gamma(k+r_2+\sigma_2+\varrho_2+1)}{\Gamma(k+\varrho_2+1)\Gamma(r_2+\sigma_2+\varrho_2+1)(r_2-k)!k!\tau^k_{end}} \frac{\partial^\nu}{\partial \tau^\nu}(\tau^k) \\ &= \sum_{k=0}^{r_2} (-1)^{r_2-k} \frac{\Gamma(r_2+\varrho_2+1)\Gamma(k+r_2+\sigma_2+\varrho_2+1)}{\Gamma(k+\varrho_2+1)\Gamma(r_2+\sigma_2+\varrho_2+1)(r_2-k)!k!\tau^k_{end}} \delta(\tau), \end{aligned} \tag{18}$$

where $\delta(\tau) = \frac{\Gamma(k+1)\tau^{k-\nu}}{\Gamma(k-\nu+1)}$.

When we differentiate, of order ν, Equation (13) with respect to τ, we obtain

$$\int_0^1 \frac{\partial^\nu}{\partial t^\nu}\Big(\mathcal{U}(\xi,\tau) - \mathcal{U}(\xi,0)\Big)d\xi = \frac{\partial^\nu}{\partial t^\nu}\Big(\mathcal{E}(\tau) - \mathcal{E}(0)\Big), \tag{19}$$

merging the previous equation with (11), we obtain

$$\frac{\partial}{\partial \xi}(\mathcal{U}(\xi,\tau))_{\xi=\xi_{end}} - \frac{\partial}{\partial \xi}(\mathcal{U}(\xi,\tau))_{\xi=0} = \frac{\partial^\nu}{\partial t^\nu}(\mathcal{E}(\tau) - \mathcal{E}(0)) - \mathcal{Q}(\tau)\int_0^1 \Delta(\xi,\tau)d\xi, \tag{20}$$

yields,

$$\mathcal{Q}(\tau) = \frac{\Theta(\tau)}{\int_0^1 \Delta(\xi,\tau)d\xi}, \tag{21}$$

where

$$\Theta(\tau)=\mathcal{E}^{(\nu)}(\tau)-\mathcal{E}^{(\nu)}(0)-\sum_{\substack{r_1=0,\ldots,\mathcal{N}\\ r_2=0,\ldots,\mathcal{M}}}\varsigma_{r_1,r_2}\widetilde{\mathcal{G}}^{\sigma_1,\varrho_1}_{\xi_{end},r_1}(1)\mathcal{G}^{\sigma_2,\varrho_2}_{\tau_{end},r_2}(\tau)+\sum_{\substack{r_1=0,\ldots,\mathcal{N}\\ r_2=0,\ldots,\mathcal{M}}}\varsigma_{r_1,r_2}\widetilde{\mathcal{G}}^{\sigma_1,\varrho_1}_{\xi_{end},r_1}(0)\mathcal{G}^{\sigma_2,\varrho_2}_{\tau_{end},r_2}(\tau),$$

and $\mathcal{E}^{(\nu)}(\tau)=\frac{\partial^{\nu}\mathcal{E}(\tau)}{\partial t^{\nu}}$. The previous derivatives of spatial and temporal variables are computed at specific nodes as

$$\begin{aligned}
\left(\frac{\partial^{\nu}}{\partial\tau^{\nu}}(\mathcal{U}(\xi,\tau))\right)^{\xi=\xi^{\sigma_1,\varrho_1,n}_{\xi_{end},\mathcal{N}},}_{\tau=\tau^{\sigma_2,\varrho_2,m}_{\tau_{end},\mathcal{M}}}&=\sum_{\substack{r_1=0,\ldots,\mathcal{N}\\ r_2=0,\ldots,\mathcal{M}}}\varsigma_{r_1,r_2}\mathcal{G}^{\sigma_1,\varrho_1}_{\xi_{end},r_1}(\xi^{\sigma_1,\varrho_1,n}_{\xi_{end},\mathcal{N}})\bar{\mathcal{G}}^{\sigma_2,\varrho_2}_{\tau_{end},r_2}(\tau^{\sigma_2,\varrho_2,m}_{\tau_{end},\mathcal{M}}),\\
\left(\frac{\partial^{\nu}}{\partial\tau^{\nu}}(\mathcal{U}(\xi,0))\right)^{\xi=\xi^{\sigma_1,\varrho_1,n}_{\xi_{end},\mathcal{N}},}_{\tau=\tau^{\sigma_2,\varrho_2,m}_{\tau_{end},\mathcal{M}}}&=\sum_{\substack{r_1=0,\ldots,\mathcal{N}\\ r_2=0,\ldots,\mathcal{M}}}\varsigma_{r_1,r_2}\mathcal{G}^{\sigma_1,\varrho_1}_{\xi_{end},r_1}(\xi^{\sigma_1,\varrho_1,n}_{\xi_{end},\mathcal{N}})\left(\frac{d^{\nu}}{d\tau^{\nu}}(\mathcal{G}^{\sigma_2,\varrho_2}_{\tau_{end},r_2}(0))\right)_{\tau=\tau^{\sigma_2,\varrho_2,m}_{\tau_{end},\mathcal{M}}},\\
\left(\frac{\partial}{\partial\xi}(\mathcal{U}_{\mathcal{N},\mathcal{M}}(\xi,\tau))\right)^{\xi=\xi_{end},}_{\tau=\tau^{\sigma_2,\varrho_2,m}_{\tau_{end},\mathcal{M}}}&=\sum_{\substack{r_1=0,\ldots,\mathcal{N}\\ r_2=0,\ldots,\mathcal{M}}}\varsigma_{r_1,r_2}\widetilde{\mathcal{G}}^{\sigma_1,\varrho_1}_{\xi_{end},r_1}(\xi_{end})\mathcal{G}^{\sigma_2,\varrho_2}_{\tau_{end},r_2}(\tau^{\sigma_2,\varrho_2,m}_{\tau_{end},\mathcal{M}}),\\
\left(\frac{\partial}{\partial\xi}(\mathcal{U}_{\mathcal{N},\mathcal{M}}(\xi,\tau))\right)^{\xi=0,}_{\tau=\tau^{\sigma_2,\varrho_2,m}_{\tau_{end},\mathcal{M}}}&=\sum_{\substack{r_1=0,\ldots,\mathcal{N}\\ r_2=0,\ldots,\mathcal{M}}}\varsigma_{r_1,r_2}\widetilde{\mathcal{G}}^{\sigma_1,\varrho_1}_{\xi_{end},r_1}(0)\mathcal{G}^{\sigma_2,\varrho_2}_{\tau_{end},r_2}(\tau^{\sigma_2,\varrho_2,m}_{\tau_{end},\mathcal{M}}),\\
\left(\frac{\partial^{2}}{\partial\xi^{2}}(\mathcal{U}(\xi,\tau))\right)^{\xi=\xi^{\sigma_1,\varrho_1,n}_{\xi_{end},\mathcal{N}}}_{\tau=\tau^{\sigma_2,\varrho_2,m}_{\tau_{end},\mathcal{M}}}&=\sum_{\substack{r_1=0,\ldots,\mathcal{N}\\ r_2=0,\ldots,\mathcal{M}}}\varsigma_{r_1,r_2}\widehat{\mathcal{G}}^{\sigma_1,\varrho_1}_{\xi_{end},r_1}(\xi^{\sigma_1,\varrho_1,n}_{\xi_{end},\mathcal{N}})\mathcal{G}^{\sigma_2,\varrho_2}_{\tau_{end},r_2}(\tau^{\sigma_2,\varrho_2,m}_{\tau_{end},\mathcal{M}}).
\end{aligned}\tag{22}$$

Additionally, we obtain

$$\mathcal{Q}(\tau^{\sigma_2,\varrho_2,m}_{\tau_{end},\mathcal{M}})=\frac{\Theta(\tau^{\sigma_2,\varrho_2,m}_{\tau_{end},\mathcal{M}})}{\int_0^1\Delta(\xi,\tau^{\sigma_2,\varrho_2,m}_{\tau_{end},\mathcal{M}})d\xi},\tag{23}$$

where $n=0,1,\cdots,\mathcal{N},\quad m=0,1,\cdots,\mathcal{M}$.

For the proposed spectral collocation technique, Equation (11) is enforced to be zero at $(\mathcal{N}-1)\times(\mathcal{M})$ points. Therefore, adapting (11)–(23), obtain linear system of algebraic equations

$$\begin{pmatrix}\aleph_{1,1}&\aleph_{1,2}&\cdots&\cdots&\aleph_{1,\mathcal{M}}\\ \aleph_{2,1}&\aleph_{2,2}&\cdots&\cdots&\aleph_{2,\mathcal{M}}\\ \cdots&\vdots&\vdots&\vdots&\cdots\\ \cdots&\vdots&\vdots&\vdots&\cdots\\ \aleph_{\mathcal{N},1}&\aleph_{\mathcal{N},2}&\cdots&\cdots&\aleph_{\mathcal{N},\mathcal{M}}\end{pmatrix}=\begin{pmatrix}\wp_{1,1}&\wp_{1,2}&\cdots&\cdots&\wp_{1,\mathcal{M}}\\ \wp_{2,1}&\wp_{2,2}&\cdots&\cdots&\wp_{2,\mathcal{M}}\\ \cdots&\vdots&\vdots&\vdots&\cdots\\ \cdots&\vdots&\vdots&\vdots&\cdots\\ \wp_{\mathcal{N},1}&\wp_{\mathcal{N},2}&\cdots&\cdots&\wp_{\mathcal{N},\mathcal{M}}\end{pmatrix}\tag{24}$$

where

$$\aleph_{n,m}=\begin{cases}\Upsilon(\xi^{\sigma_1,\varrho_1,n}_{\xi_{end}\mathcal{N}},\tau^{\sigma_2,\varrho_2,m}_{\tau_{end},\mathcal{M}}), & n=1,\cdots,\mathcal{N}-1, \quad m=1,\cdots,\mathcal{M};\\ \sum_{\substack{r_1=0,\ldots,\mathcal{N}\\ r_2=0,\ldots,\mathcal{M}}}\varsigma_{r_1,r_2}\mathcal{G}^{\sigma_1,\varrho_1}_{\xi_{end},r_1}(\xi^{\sigma_1,\varrho_1,n}_{\xi_{end}\mathcal{N}})\mathcal{G}^{\sigma_2,\varrho_2}_{\tau_{end},r_2}(0), & m=0,\ n=1,\cdots,\mathcal{N}-1;\\ \sum_{\substack{r_1=0,\ldots,\mathcal{N}\\ r_2=0,\ldots,\mathcal{M}}}\varsigma_{r_1,r_2}\mathcal{G}^{\sigma_1,\varrho_1}_{\xi_{end},r_1}(0)\mathcal{G}^{\sigma_2,\varrho_2}_{\tau_{end},r_2}(\tau^{\sigma_2,\varrho_2,m}_{\tau_{end},\mathcal{M}}), & n=0,\ m=0,\cdots,\mathcal{M};\\ \sum_{\substack{r_1=0,\ldots,\mathcal{N}\\ r_2=0,\ldots,\mathcal{M}}}\varsigma_{r_1,r_2}\mathcal{G}^{\sigma_1,\varrho_1}_{\xi_{end},r_1}(\xi_{end})\mathcal{G}^{\sigma_2,\varrho_2}_{\tau_{end},r_2}(\tau^{\sigma_2,\varrho_2,m}_{\tau_{end},\mathcal{M}}), & n=\mathcal{N},=0,\cdots,\mathcal{M}.\end{cases}$$

$$\wp_{n,m}=\begin{cases}\dfrac{\Theta(\tau^{\sigma_2,\varrho_2,m}_{\tau_{end},\mathcal{M}})}{\int_0^1\Delta(\xi,\tau^{\sigma_2,\varrho_2,m}_{\tau_{end},\mathcal{M}})d\xi}\Delta(\xi^{\sigma_1,\varrho_1,n}_{\xi_{end}\mathcal{N}},\tau^{\sigma_2,\varrho_2,m}_{\tau_{end},\mathcal{M}}), & n=1,\cdots,\mathcal{N}-1, \quad m=1,\cdots,\mathcal{M};\\ \lambda_1(\xi^{\sigma_1,\varrho_1,n}_{\xi_{end}\mathcal{N}}), & m=0,\ n=1,\cdots,\mathcal{N}-1;\\ \lambda_2(\tau^{\sigma_2,\varrho_2,m}_{\tau_{end},\mathcal{M}}), & n=0,\ m=0,\cdots,\mathcal{M};\\ \lambda_3(\tau^{\sigma_2,\varrho_2,m}_{\tau_{end},\mathcal{M}}), & n=\mathcal{N},=0,\cdots,\mathcal{M}.\end{cases}$$

where

$$\begin{aligned}\Upsilon(\xi^{\sigma_1,\varrho_1,n}_{\xi_{end}\mathcal{N}},\tau^{\sigma_2,\varrho_2,m}_{\tau_{end},\mathcal{M}}) = & \sum_{\substack{r_1=0,\ldots,\mathcal{N}\\ r_2=0,\ldots,\mathcal{M}}}\varsigma_{r_1,r_2}\mathcal{G}^{\sigma_1,\varrho_1}_{\xi_{end},r_1}(\xi^{\sigma_1,\varrho_1,n}_{\xi_{end}\mathcal{N}})\tilde{\mathcal{G}}^{\sigma_2,\varrho_2}_{\tau_{end},r_2}(\tau^{\sigma_2,\varrho_2,m}_{\tau_{end},\mathcal{M}})-\\ & \sum_{\substack{r_1=0,\ldots,\mathcal{N}\\ r_2=0,\ldots,\mathcal{M}}}\varsigma_{r_1,r_2}\mathcal{G}^{\sigma_1,\varrho_1}_{\xi_{end},r_1}(\xi^{\sigma_1,\varrho_1,n}_{\xi_{end}\mathcal{N}})\left(\frac{d^\nu}{d\tau^\nu}(\mathcal{G}^{\sigma_2,\varrho_2}_{\tau_{end},r_2}(0))\right)_{\tau=\tau^{\sigma_2,\varrho_2,m}_{\tau_{end},\mathcal{M}}}-\\ & \sum_{\substack{r_1=0,\ldots,\mathcal{N}\\ r_2=0,\ldots,\mathcal{M}}}\varsigma_{r_1,r_2}\widehat{\mathcal{G}}^{\sigma_1,\varrho_1}_{\xi_{end},r_1}(\xi^{\sigma_1,\varrho_1,n}_{\xi_{end}\mathcal{N}})\mathcal{G}^{\sigma_2,\varrho_2}_{\tau_{end},r_2}(\tau^{\sigma_2,\varrho_2,m}_{\tau_{end},\mathcal{M}}).\end{aligned}$$

3.2. Nonlocal Conditions

Here, we develop a numerical scheme to deal with the time-fractional IHEs of the form

$$\frac{\partial^\nu}{\partial t^\nu}\Big(\mathcal{U}(\xi,\tau)-\mathcal{U}(\xi,0)\Big)=\frac{\partial^2}{\partial x^2}(\mathcal{U}(\xi,\tau))+\mathcal{Q}(\tau)\Delta(\xi,\tau), \quad (\xi,\tau)\in\Lambda^\bullet\times\Lambda^\diamond, \tag{25}$$

$$\begin{gathered}\mathcal{U}(\xi,0)=\lambda_1(\xi), \quad \xi\in\Lambda^\bullet,\\ \mathcal{U}(0,\tau)+\alpha_1\mathcal{U}(\xi_{end},\tau)=\lambda_2(\tau), \quad \mathcal{U}_\xi(0,\tau)+\alpha_2\mathcal{U}(\xi_{end},\tau)=\lambda_3(\tau), \quad \tau\in\Lambda^\diamond,\end{gathered} \tag{26}$$

where $\Lambda^\bullet\equiv[0,\xi_{end}]$, $\Lambda^\diamond\equiv[0,\tau_{end}]$, $\mathcal{U}(\xi,\tau)$ and $\mathcal{Q}(\tau)$ are unknown functions, while $\Delta(\xi,\tau)$ is a given one. The energy condition is given by

$$\int_0^1\mathcal{U}(\xi,\tau)d\xi=\mathcal{E}(\tau). \tag{27}$$

Using the previous results, we obtain the following linear system of algebraic equations

$$\begin{pmatrix}\aleph_{1,1} & \aleph_{1,2} & \cdots & \cdots & \aleph_{1,\mathcal{M}}\\ \aleph_{2,1} & \aleph_{2,2} & \cdots & \cdots & \aleph_{2,\mathcal{M}}\\ \cdots & \vdots & \vdots & \vdots & \cdots\\ \cdots & \vdots & \vdots & \vdots & \cdots\\ \aleph_{\mathcal{N},1} & \aleph_{\mathcal{N},2} & \cdots & \cdots & \aleph_{\mathcal{N},\mathcal{M}}\end{pmatrix}=\begin{pmatrix}\wp_{1,1} & \wp_{1,2} & \cdots & \cdots & \wp_{1,\mathcal{M}}\\ \wp_{2,1} & \wp_{2,2} & \cdots & \cdots & \wp_{2,\mathcal{M}}\\ \cdots & \vdots & \vdots & \vdots & \cdots\\ \cdots & \vdots & \vdots & \vdots & \cdots\\ \wp_{\mathcal{N},1} & \wp_{\mathcal{N},2} & \cdots & \cdots & \wp_{\mathcal{N},\mathcal{M}}\end{pmatrix}, \tag{28}$$

where

$$\aleph_{n,m} = \begin{cases} \Upsilon(\xi^{\sigma_1,\varrho_1,n}_{\xi_{end}\mathcal{N}}, \tau^{\sigma_2,\varrho_2,m}_{\tau_{end},\mathcal{M}}), & n = 1,\cdots,\mathcal{N}-1, \quad m = 1,\cdots,\mathcal{M}; \\ \sum_{\substack{r_1=0,\ldots,\mathcal{N}\\ r_2=0,\ldots,\mathcal{M}}} \varsigma_{r_1,r_2} \mathcal{G}^{\sigma_1,\varrho_1}_{\xi_{end},r_1}(\xi^{\sigma_1,\varrho_1,n}_{\xi_{end}\mathcal{N}}) \mathcal{G}^{\sigma_2,\varrho_2}_{\tau_{end},r_2}(0), & m = 0,\ n = 1,\cdots,\mathcal{N}-1; \\ \sum_{\substack{r_1=0,\ldots,\mathcal{N}\\ r_2=0,\ldots,\mathcal{M}}} \varsigma_{r_1,r_2} \mathcal{G}^{\sigma_1,\varrho_1}_{\xi_{end},r_1}(0) \mathcal{G}^{\sigma_2,\varrho_2}_{\tau_{end},r_2}(\tau^{\sigma_2,\varrho_2,m}_{\tau_{end},\mathcal{M}}) + & \\ \alpha_1 \sum_{\substack{r_1=0,\ldots,\mathcal{N}\\ r_2=0,\ldots,\mathcal{M}}} \varsigma_{r_1,r_2} \mathcal{G}^{\sigma_1,\varrho_1}_{\xi_{end},r_1}(\xi_{end}) \mathcal{G}^{\sigma_2,\varrho_2}_{\tau_{end},r_2}(\tau^{\sigma_2,\varrho_2,m}_{\tau_{end},\mathcal{M}}), & n = 0,\ m = 0,\cdots,\mathcal{M}; \\ \sum_{\substack{r_1=0,\ldots,\mathcal{N}\\ r_2=0,\ldots,\mathcal{M}}} \varsigma_{r_1,r_2} \widetilde{\mathcal{G}}^{\sigma_1,\varrho_1}_{\xi_{end},r_1}(0) \mathcal{G}^{\sigma_2,\varrho_2}_{\tau_{end},r_2}(\tau^{\sigma_2,\varrho_2,m}_{\tau_{end},\mathcal{M}}) + & \\ \alpha_2 \sum_{\substack{r_1=0,\ldots,\mathcal{N}\\ r_2=0,\ldots,\mathcal{M}}} \varsigma_{r_1,r_2} \mathcal{G}^{\sigma_1,\varrho_1}_{\xi_{end},r_1}(0) \mathcal{G}^{\sigma_2,\varrho_2}_{\tau_{end},r_2}(\tau^{\sigma_2,\varrho_2,m}_{\tau_{end},\mathcal{M}}), & n = \mathcal{N}, = 0,\cdots,\mathcal{M}. \end{cases}$$

$$\wp_{n,m} = \begin{cases} \frac{\Theta(\tau^{\sigma_2,\varrho_2,m}_{\tau_{end},\mathcal{M}})}{\int_0^1 \Delta(\xi,\tau^{\sigma_2,\varrho_2,m}_{\tau_{end},\mathcal{M}}) d\xi} \Delta(\xi^{\sigma_1,\varrho_1,n}_{\xi_{end}\mathcal{N}}, \tau^{\sigma_2,\varrho_2,m}_{\tau_{end},\mathcal{M}}), & n = 1,\cdots,\mathcal{N}-1, \quad m = 1,\cdots,\mathcal{M}; \\ \lambda_1(\xi^{\sigma_1,\varrho_1,n}_{\xi_{end}\mathcal{N}}), & m = 0,\ n = 1,\cdots,\mathcal{N}-1; \\ \lambda_2(\tau^{\sigma_2,\varrho_2,m}_{\tau_{end},\mathcal{M}}), & n = 0,\ m = 0,\cdots,\mathcal{M}; \\ \lambda_3(\tau^{\sigma_2,\varrho_2,m}_{\tau_{end},\mathcal{M}}), & n = \mathcal{N}, = 0,\cdots,\mathcal{M}. \end{cases}$$

where

$$\begin{aligned} \Upsilon(\xi^{\sigma_1,\varrho_1,n}_{\xi_{end}\mathcal{N}}, \tau^{\sigma_2,\varrho_2,m}_{\tau_{end},\mathcal{M}}) = & \sum_{\substack{r_1=0,\ldots,\mathcal{N}\\ r_2=0,\ldots,\mathcal{M}}} \varsigma_{r_1,r_2} \mathcal{G}^{\sigma_1,\varrho_1}_{\xi_{end},r_1}(\xi^{\sigma_1,\varrho_1,n}_{\xi_{end}\mathcal{N}}) \widetilde{\mathcal{G}}^{\sigma_2,\varrho_2}_{\tau_{end},r_2}(\tau^{\sigma_2,\varrho_2,m}_{\tau_{end},\mathcal{M}}) - \\ & \sum_{\substack{r_1=0,\ldots,\mathcal{N}\\ r_2=0,\ldots,\mathcal{M}}} \varsigma_{r_1,r_2} \mathcal{G}^{\sigma_1,\varrho_1}_{\xi_{end},r_1}(\xi^{\sigma_1,\varrho_1,n}_{\xi_{end}\mathcal{N}}) \left(\frac{d^\nu}{d\tau^\nu} (\mathcal{G}^{\sigma_2,\varrho_2}_{\tau_{end},r_2}(0)) \right)_{\tau=\tau^{\sigma_2,\varrho_2,m}_{\tau_{end},\mathcal{M}}} - \\ & \sum_{\substack{r_1=0,\ldots,\mathcal{N}\\ r_2=0,\ldots,\mathcal{M}}} \varsigma_{r_1,r_2} \widehat{\mathcal{G}}^{\sigma_1,\varrho_1}_{\xi_{end},r_1}(\xi^{\sigma_1,\varrho_1,n}_{\xi_{end}\mathcal{N}}) \mathcal{G}^{\sigma_2,\varrho_2}_{\tau_{end},r_2}(\tau^{\sigma_2,\varrho_2,m}_{\tau_{end},\mathcal{M}}). \end{aligned}$$

$$\Upsilon(\xi^{\sigma_1,\varrho_1,n}_{\xi_{end}\mathcal{N}}, \tau^{\sigma_2,\varrho_2,m}_{\tau_{end},\mathcal{M}}) = \frac{\Theta(\tau^{\sigma_2,\varrho_2,m}_{\tau_{end},\mathcal{M}})}{\int_0^1 \Delta(\xi,\tau^{\sigma_2,\varrho_2,m}_{\tau_{end},\mathcal{M}}) d\xi} \Delta(\xi^{\sigma_1,\varrho_1,n}_{\xi_{end}\mathcal{N}}, \tau^{\sigma_2,\varrho_2,m}_{\tau_{end},\mathcal{M}}), \tag{29}$$

4. Numerical Results

This section is devoted to providing some numerical results to show the robustness and the accuracy of the spectral collocation schemes presented in this work.

Example 1. *We consider the following IHEs*

$$\begin{aligned} \frac{\partial^\nu}{\partial t^\nu}\Big(\mathcal{U}(\xi,\tau) - \mathcal{U}(\xi,0)\Big) =& \frac{\partial^2}{\partial x^2}(\mathcal{U}(\xi,\tau)) + \mathcal{Q}(\tau) e^{-\tau^2} \sin(\pi\xi) \left(\frac{2(-\nu+\tau+2)\tau^{1-\nu}}{\Gamma(3-\nu)} + \pi^2(\tau+1)^2 \right), \\ & (\xi,\tau) \in [0,1] \times [0,1], \end{aligned} \tag{30}$$

with the local conditions

$$\begin{aligned} \mathcal{U}(\xi,0) = \sin(\pi\xi), \quad \xi \in [0,1], \\ \mathcal{U}(0,\tau) = 0, \quad \mathcal{U}(1,\tau) = 0, \quad \tau \in [0,1], \end{aligned} \tag{31}$$

and the extra energy condition

$$\int_0^1 \mathcal{U}(\xi,\tau) d\xi = \frac{2(\tau+1)^2}{\pi}, \tag{32}$$

the exact solution and unknown source function are given by $\mathcal{U}(\xi,\tau) = (\tau+1)^2 \sin(\pi\xi)$, $\mathcal{Q}(\tau) = e^{\tau^2}$.

The absolute errors $E_{\mathcal{U}}$ and $E_{\mathcal{Q}}$ are defined as

$$E_{\mathcal{U}}(\xi,\tau) = |\mathcal{U}(\xi,\tau) - \mathcal{U}_{Approx}(\xi,\tau)|,$$
$$E_{\mathcal{Q}}(\tau) = |\mathcal{Q}(\tau) - \mathcal{Q}_{Approx}(\tau)|.$$

Moreover, the maximum absolute errors $M_{E_{\mathcal{U}}}$ and $M_{E_{\mathcal{Q}}}$ are defined as

$$M_{E_{\mathcal{U}}} = MAXE_{\mathcal{U}}(\xi,\tau)(\xi,\tau) \in \Lambda^{\bullet} \times \Lambda^{\diamond},$$
$$M_{E_{\mathcal{Q}}} = MAXE_{\mathcal{Q}}(\tau)\tau \in \Lambda^{\diamond}.$$

Tables 1 and 2 provide the maximum absolute errors $M_{E_{\mathcal{U}}}$ and $M_{E_{\mathcal{Q}}}$ of the approximate solution at various values of parameters. From these results, the proposed scheme provides better numerical results. It is also observed that excellent approximations with a few collocation points are achieved. In Figures 1 and 2, with values of parameters listed in their captions, the numerical solution and its absolute errors functions are displayed, respectively. Additionally, the exact and approximate solutions are readily displayed in Figures 3 and 4 for $\mathcal{Q}(\tau)$ and temperature function $\mathcal{U}(\xi,\tau)$, respectively. However, absolute errors functions of the temperature and $\mathcal{Q}(\tau)$ are displayed in Figures 5–7. Moreover, rate of convergence is displayed in Figures 8 and 9. The exponential convergence of our method is observed in these graphs.

Table 1. $M_{E_{\mathcal{U}}}$ for problem (30).

ν	$(\mathcal{N},\mathcal{M})$	CPU Time	(0, 0, 0, 0)	(0, −0.5, 0, 0.5)	(−0.5, −0.5, 0, 0)	(−0.5, −0.5, 0.5, 0.5)
0.5	(4,4)	3.874	5.54207×10^{-1}	4.50114×10^{-1}	3.30903×10^{-1}	3.30301×10^{-1}
	(8,8)	10.937	1.069×10^{-4}	7.62826×10^{-5}	4.23773×10^{-5}	4.23533×10^{-5}
	(12,12)	55.062	2.84348×10^{-9}	1.93179×10^{-9}	9.20255×10^{-10}	9.20021×10^{-10}
	(16,16)	232.329	6.33922×10^{-14}	9.6867×10^{-14}	3.18634×10^{-14}	9.12603×10^{-14}
0.9	(4,4)	5.751	4.51528×10^{-1}	1.78626×10^{-1}	2.64455×10^{-1}	2.64435×10^{-1}
	(8,8)	12.657	8.30291×10^{-5}	5.92663×10^{-5}	3.28873×10^{-5}	328844×10^{-5}
	(12,12)	61.278	2.20829×10^{-9}	1.50057×10^{-9}	7.14412×10^{-10}	7.14381×10^{-10}
	(16,16)	239.312	2.17604×10^{-14}	1.3467×10^{-13}	5.29576×10^{-14}	6.1945×10^{-14}
1.0	(4,4)	3.39	4.24550×10^{-1}	3.41265×10^{-1}	2.47565×10^{-1}	2.476208×10^{-1}
	(8,8)	8.812	7.71774×10^{-5}	5.510238×10^{-5}	3.05607×10^{-5}	3.05625×10^{-5}
	(12,12)	58.25	2.05212×10^{-9}	1.39463×10^{-9}	6.638062×10^{-10}	6.63822×10^{-10}
	(16,16)	235.514	1.5614×10^{-14}	1.02934×10^{-14}	4.37859×10^{-15}	4.378644×10^{-15}

Table 2. $M_{E_{\mathcal{Q}}}$ for problem (30).

ν	$(\mathcal{N},\mathcal{M})$	(0, 0, 0, 0)	(0, −0.5, 0, 0.5)	(−0.5, −0.5, 0, 0)	(−0.5, −0.5, 0.5, 0.5)
0.5	(4,4)	2.37763×10^{-1}	1.93756×10^{-1}	1.47532×10^{-1}	1.47488×10^{-1}
	(8,8)	5.79538×10^{-5}	4.13846×10^{-5}	2.31711×10^{-5}	2.3159×10^{-5}
	(12,12)	1.68474×10^{-9}	1.1447×10^{-9}	5.47435×10^{-10}	5.47225×10^{-10}
	(16,16)	1.83853×10^{-13}	5.48228×10^{-13}	1.16351×10^{-13}	1.28564×10^{-13}
0.9	(4,4)	1.84722×10^{-1}	1.49677×10^{-1}	1.13969×10^{-1}	1.13951×10^{-1}
	(8,8)	4.46693×10^{-5}	3.19146×10^{-5}	1.78888×10^{-5}	1.78816×10^{-5}
	(12,12)	1.31451×10^{-9}	8.93408×10^{-10}	4.27471×10^{-10}	4.27336×10^{-10}
	(16,16)	1.7919×10^{-13}	3.80598×10^{-14}	2.26041×10^{-13}	2.14051×10^{-13}
1.0	(4,4)	1.725×10^{-1}	1.39696×10^{-1}	1.06467×10^{-1}	1.06484×10^{-1}
	(8,8)	4.16394×10^{-5}	2.97589×10^{-5}	1.66843×10^{-5}	1.66798×10^{-5}
	(12,12)	1.22865×10^{-9}	8.35128×10^{-10}	3.99611×10^{-10}	3.99526×10^{-10}
	(16,16)	9.76996×10^{-15}	6.21725×10^{-15}	2.66454×10^{-15}	2.66454×10^{-15}

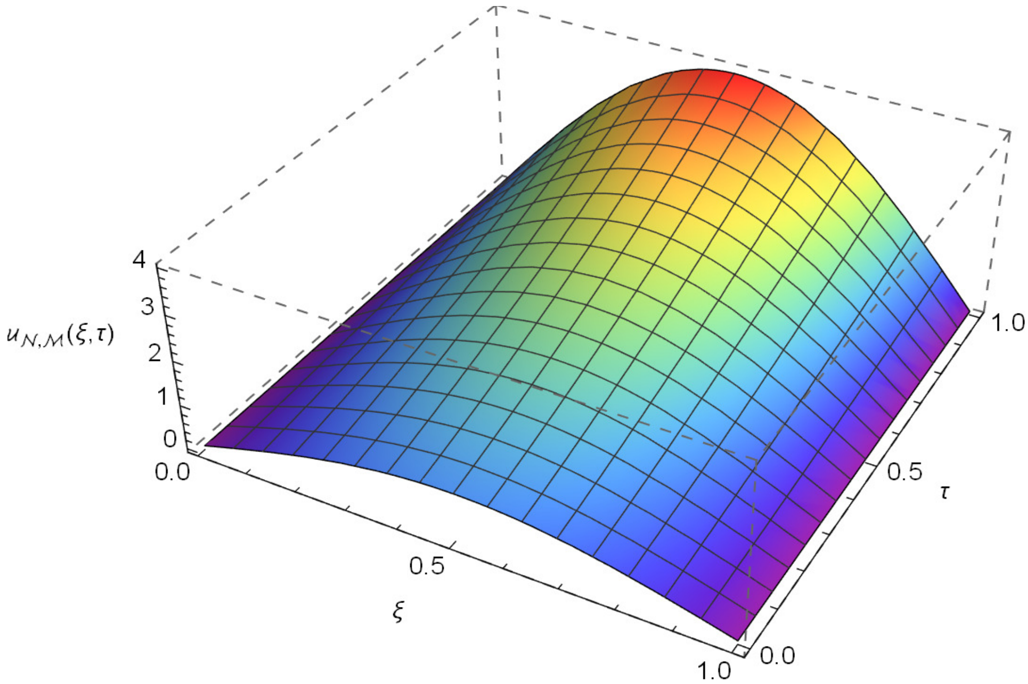

Figure 1. Numerical solution of the problem (30), where $\sigma_1 = \varrho_1 = \sigma_2 = \varrho_2 = 0$, $\nu = 0.5$ and $\mathcal{N} = \mathcal{M} = 16$.

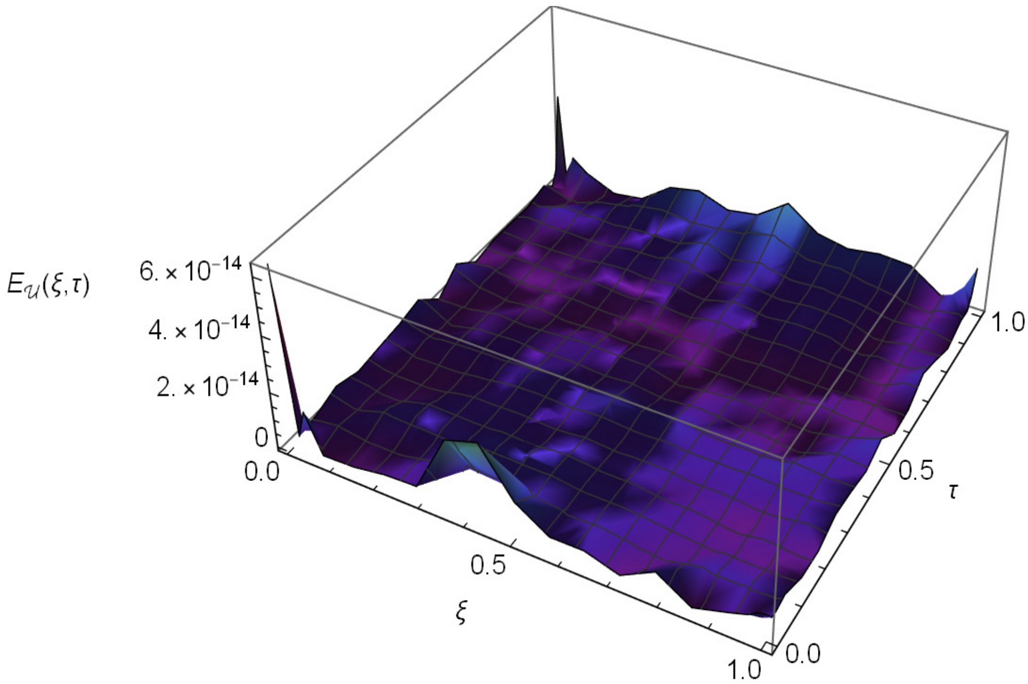

Figure 2. Absolute errors graph of the problem (30), where $\sigma_1 = \varrho_1 = \sigma_2 = \varrho_2 = 0$, $\nu = 0.5$ and $\mathcal{N} = \mathcal{M} = 16$.

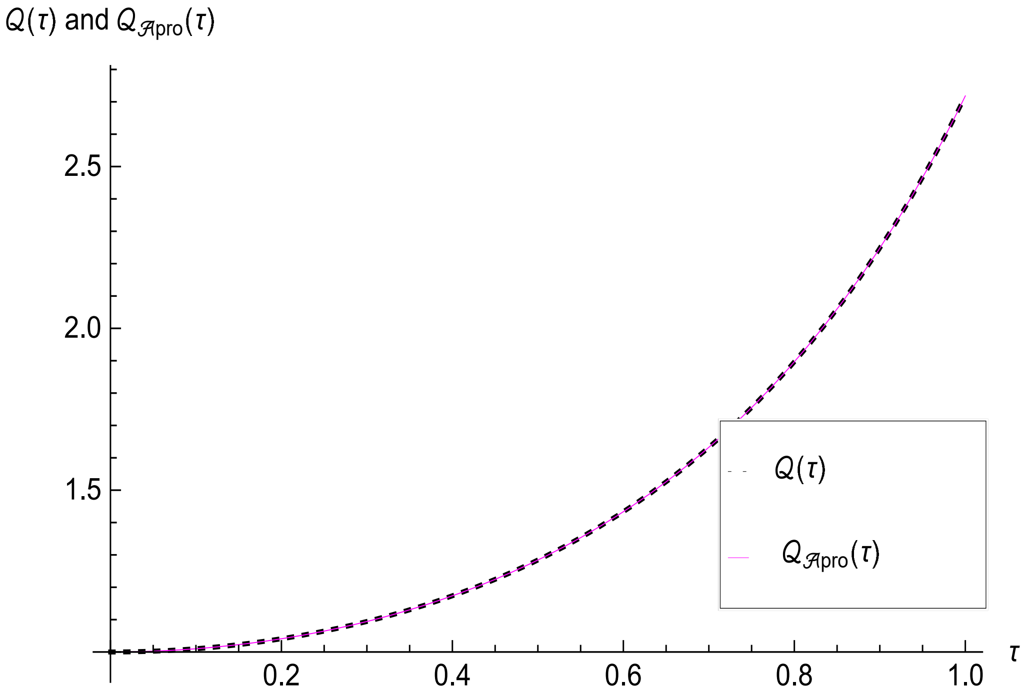

Figure 3. Curves of the exact and numerical solutions of $\mathcal{Q}(\tau)$ of the problem (30), where $\sigma_1 = \varrho_1 = \sigma_2 = \varrho_2 = 0$, $\nu = 0.5$ and $\mathcal{N} = \mathcal{M} = 16$.

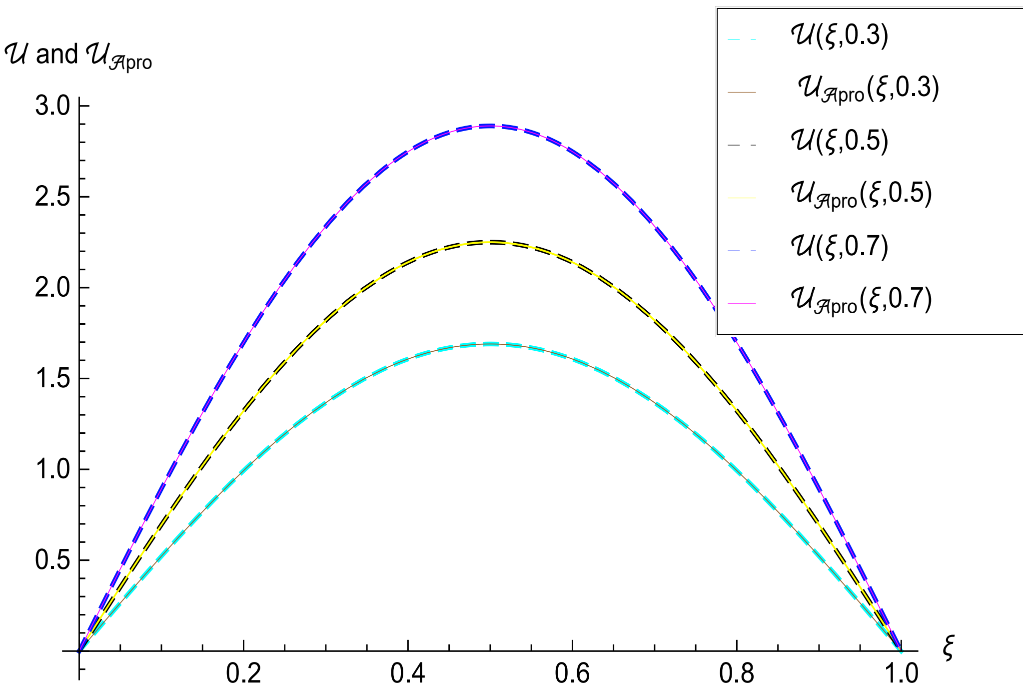

Figure 4. x-Curves of the exact and numerical solutions of $\mathcal{U}(\xi, \tau)$ of the problem (30), where $\sigma_1 = \varrho_1 = \sigma_2 = \varrho_2 = 0$, $\nu = 0.5$ and $\mathcal{N} = \mathcal{M} = 16$.

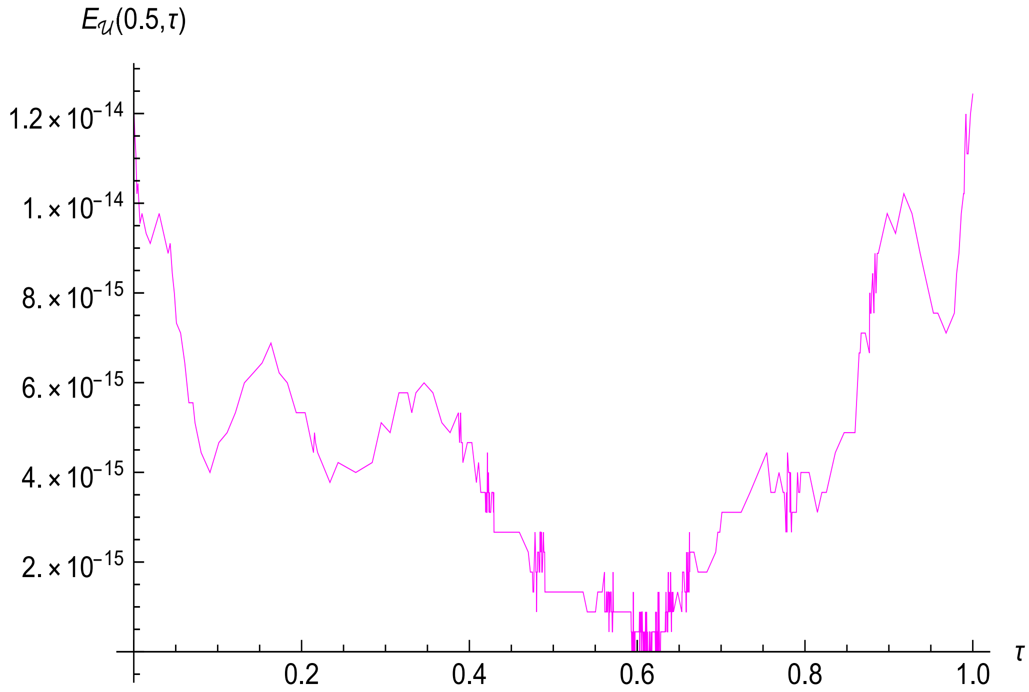

Figure 5. τ-Absolute errors $E_{\mathcal{U}}(0.5,\tau)$ graph of the problem (30), where $\sigma_1 = \varrho_1 = \sigma_2 = \varrho_2 = 0$, $\nu = 0.5$ and $\mathcal{N} = \mathcal{M} = 16$.

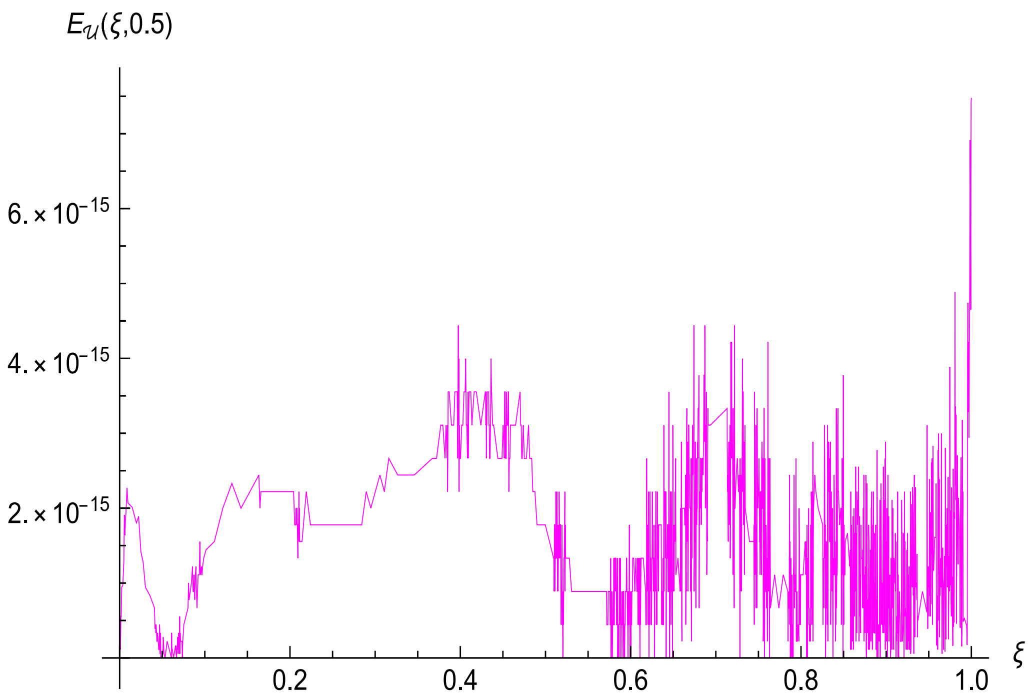

Figure 6. ξ-Absolute errors graph $E_{\mathcal{U}}(\xi, 0.5)$of the problem (30), where $\sigma_1 = \varrho_1 = \sigma_2 = \varrho_2 = 0$, $\nu = 0.5$ and $\mathcal{N} = \mathcal{M} = 16$.

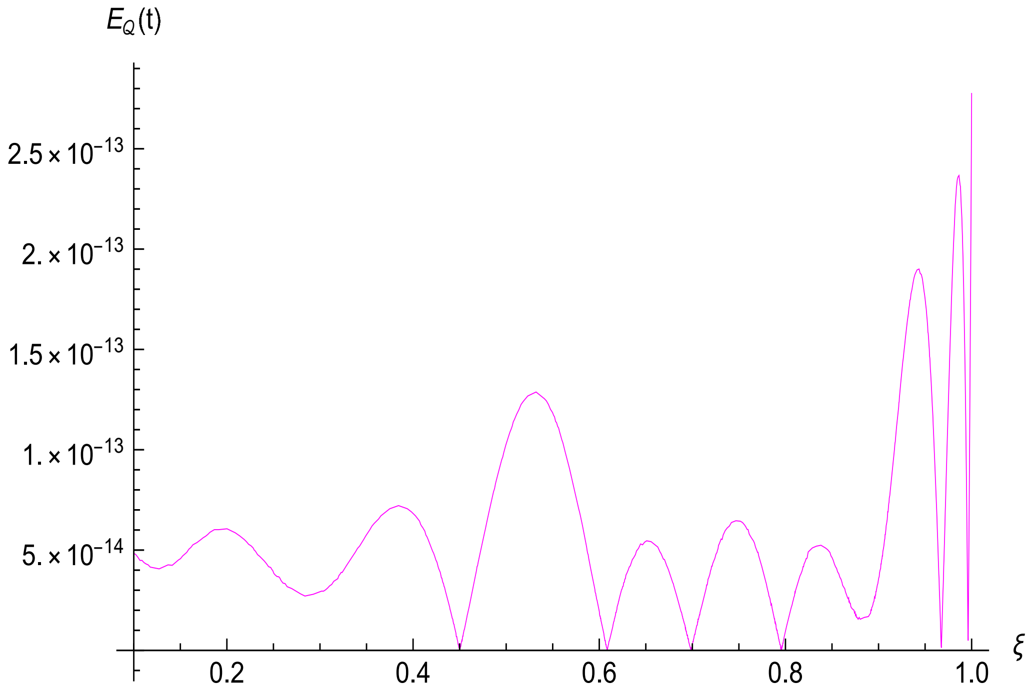

Figure 7. Absolute errors $E_{\mathcal{Q}}(\tau)$ graph of the problem (30), where $\sigma_1 = \varrho_1 = \sigma_2 = \varrho_2 = 0$, $\nu = 0.5$ and $\mathcal{N} = \mathcal{M} = 16$.

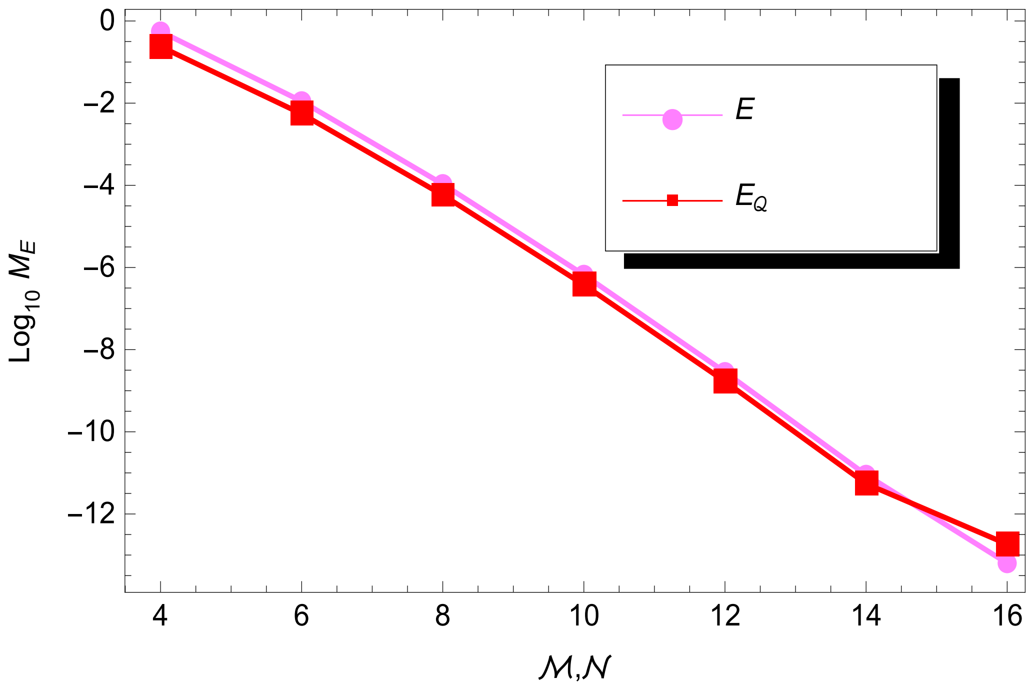

Figure 8. M_E convergence of problem (30), where $\sigma_1 = \varrho_1 = \sigma_2 = \varrho_2 = 0$, $\nu = 0.5$.

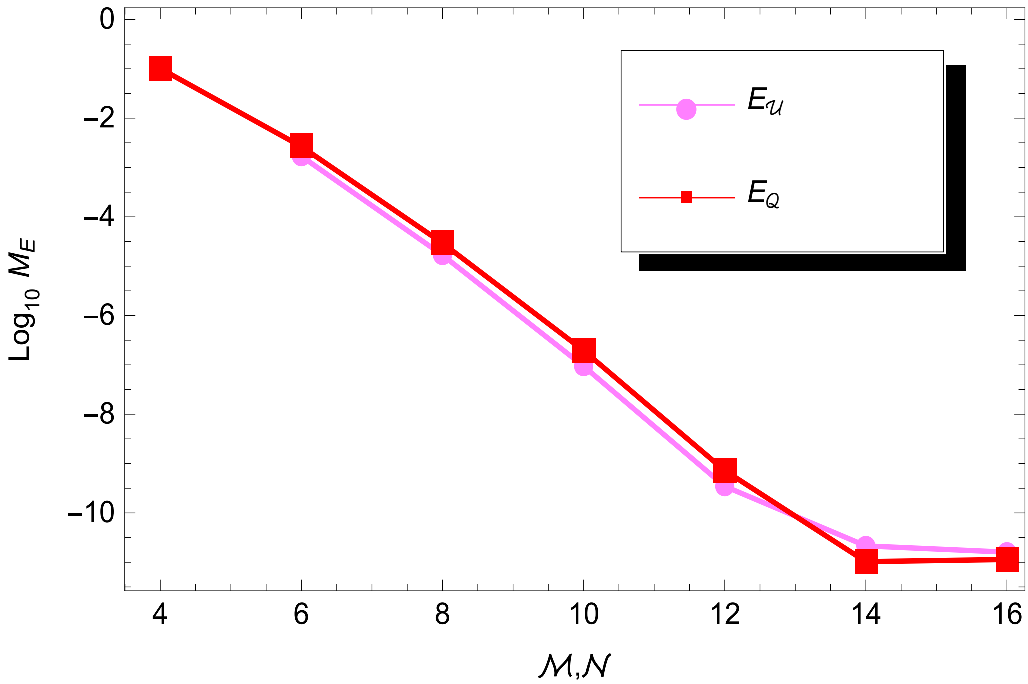

Figure 9. M_E convergence of problem (30), where $\sigma_1 = \varrho_1 = -0.5$, $\sigma_2 = \varrho_2 = 0.5$, $\nu = 0.9$.

Example 2. *We consider the IHEs*

$$\frac{\partial^{\nu}}{\partial t^{\nu}}\Big(\mathcal{U}(\xi,\tau) - \mathcal{U}(\xi,0)\Big) = \frac{\partial^2}{\partial x^2}(\mathcal{U}(\xi,\tau)) + \mathcal{Q}(\tau)\cos\left(\pi\left(\xi + \frac{1}{4}\right)\right)\left(\frac{2\tau^{-\nu}}{\Gamma(3-\nu)} + \pi^2\right), \quad (\xi,\tau) \in [0,1]\times[0,1], \tag{33}$$

with the nonlocal conditions

$$\begin{gathered} \mathcal{U}(\xi,0) = \sin(\pi\xi), \quad \xi \in [0,1], \\ \mathcal{U}(0,\tau) = \mathcal{U}(1,\tau), \quad \frac{\partial}{\partial x}\Big(\mathcal{U}(\xi,\tau)\Big)_{\xi=0} + \pi\mathcal{U}(0,\tau) = 0, \quad \tau \in [0,1], \end{gathered} \tag{34}$$

and the extra energy condition

$$\int_0^1 \mathcal{U}(\xi,\tau)d\xi = -\frac{\sqrt{2}\tau^2}{\pi}, \tag{35}$$

the exact solution and unknown source function are given by $\mathcal{U}(\xi,\tau) = \tau^2\cos\left(\pi\xi + \frac{\pi}{4}\right)$, $\mathcal{Q}(\tau) = \tau^2$.

Tables 3 and 4 display the maximum absolute errors $M_{E_{\mathcal{U}}}$ and $M_{E_{\mathcal{Q}}}$ of the approximate solution at different values of parameters, respectively. In Figures 10 and 11, with values of parameters listed in their captions, numerical solution and absolute errors graphs are displayed, respectively. Additionally, the exact and approximate solutions are displayed in Figures 12 and 13 for $\mathcal{Q}(\tau)$ and temperature function $\mathcal{U}(\xi,\tau)$, respectively. However, absolute errors curves of the temperature and $\mathcal{Q}(\tau)$ functions are displayed in Figures 14–16.

Table 3. $M_{E_{\mathcal{U}}}$ for problem (33).

ν	$(\mathcal{N},\mathcal{M})$	(0, 0, 0, 0)	(0, −0.5, 0, 0.5)	(−0.5, −0.5, 0, 0)	(−0.5, −0.5, 0.5, 0.5)
0.5	(4,4)	1.27607×10^{-1}	3.15438×10^{-2}	8.46812×10^{-2}	8.46738×10^{-2}
	(8,8)	4.7083×10^{-5}	3.90995×10^{-5}	1.91081×10^{-5}	1.91082×10^{-5}
	(12,12)	1.66851×10^{-9}	1.97664×10^{-9}	5.41362×10^{-10}	5.41373×10^{-10}
	(16,16)	2.0849×10^{-14}	3.87468×10^{-14}	1.69864×10^{-14}	3.38618×10^{-14}
0.9	(4,4)	1.17572×10^{-1}	3.60552×10^{-2}	7.75196×10^{-2}	7.74936×10^{-2}
	(8,8)	4.15201×10^{-5}	2.09117×10^{-5}	1.65554×10^{-5}	1.67636×10^{-5}
	(12,12)	1.63111×10^{-9}	1.97664×10^{-9}	5.35284×10^{-10}	3.46596×10^{-10}
	(16,16)	9.74665×10^{-11}	7.43456×10^{-11}	1.87779×10^{-10}	1.60306×10^{-11}

Table 4. $M_{E_{\mathcal{Q}}}$ for problem (33).

ν	$(\mathcal{N},\mathcal{M})$	(0, 0, 0, 0)	(0, −0.5, 0, 0.5)	(−0.5, −0.5, 0, 0)	(−0.5, −0.5, 0.5, 0.5)
0.5	(4,4)	1.81999×10^{-1}	6.99633×10^{-3}	1.22372×10^{-1}	0.122373×10^{-1}
	(8,8)	8.67215×10^{-5}	4.68354×10^{-5}	3.46128×10^{-5}	3.46127×10^{-5}
	(12,12)	3.25847×10^{-9}	2.82092×10^{-9}	1.05757×10^{-9}	1.05754×10^{-9}
	(16,16)	7.70495×10^{-14}	6.28386×10^{-14}	4.31877×10^{-14}	4.75175×10^{-14}
0.9	(4,4)	1.52889×10^{-1}	2.92712×10^{-2}	1.01293×10^{-1}	1.0128×10^{-1}
	(8,8)	7.33228×10^{-5}	1.97339×10^{-5}	2.9295×10^{-5}	2.93316×10^{-5}
	(12,12)	2.13166×10^{-9}	2.82092×10^{-9}	6.91775×10^{-10}	7.22927×10^{-10}
	(16,16)	6.70036×10^{-11}	5.29218×10^{-11}	1.33594×10^{-10}	1.13941×10^{-11}

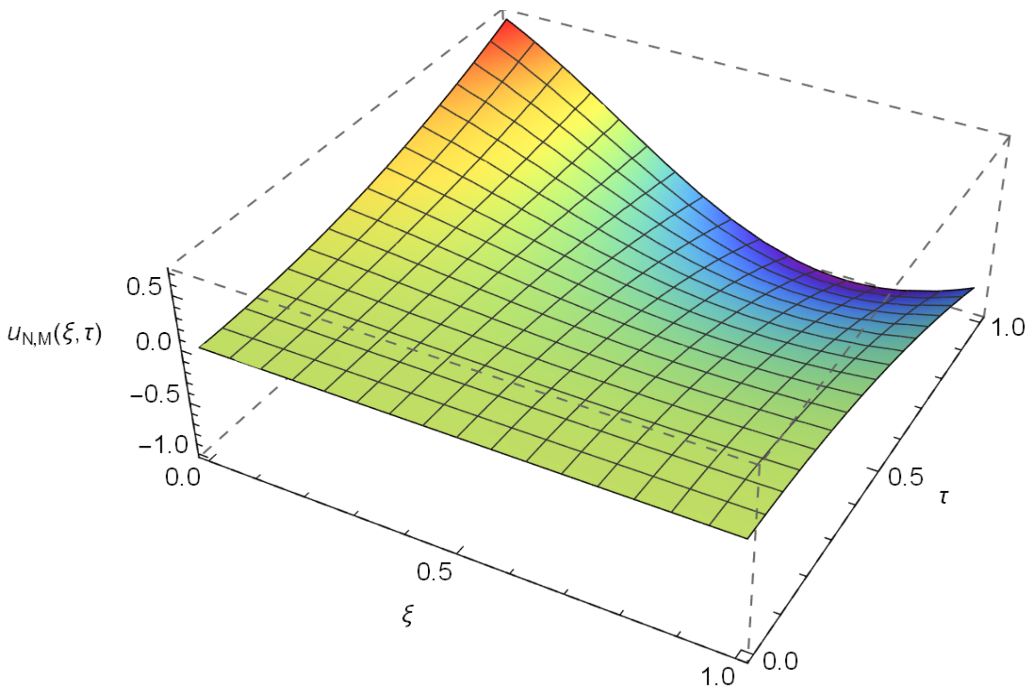

Figure 10. Numerical solution of the problem (33), where $\sigma_1 = \varrho_1 = \sigma_2 = \varrho_2 = 0$, $\nu = 0.9$ and $\mathcal{N} = \mathcal{M} = 16$.

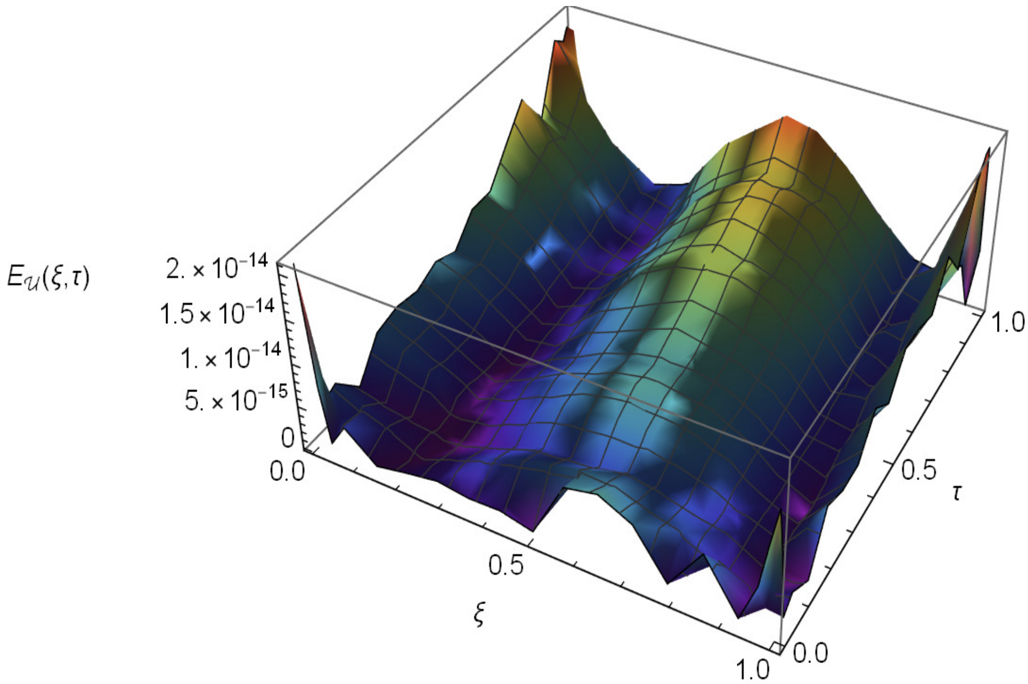

Figure 11. Absolute errors graph of the problem (33),where $\sigma_1 = \varrho_1 = \sigma_2 = \varrho_2 = 0$, $\nu = 0.9$ and $\mathcal{N} = \mathcal{M} = 16$.

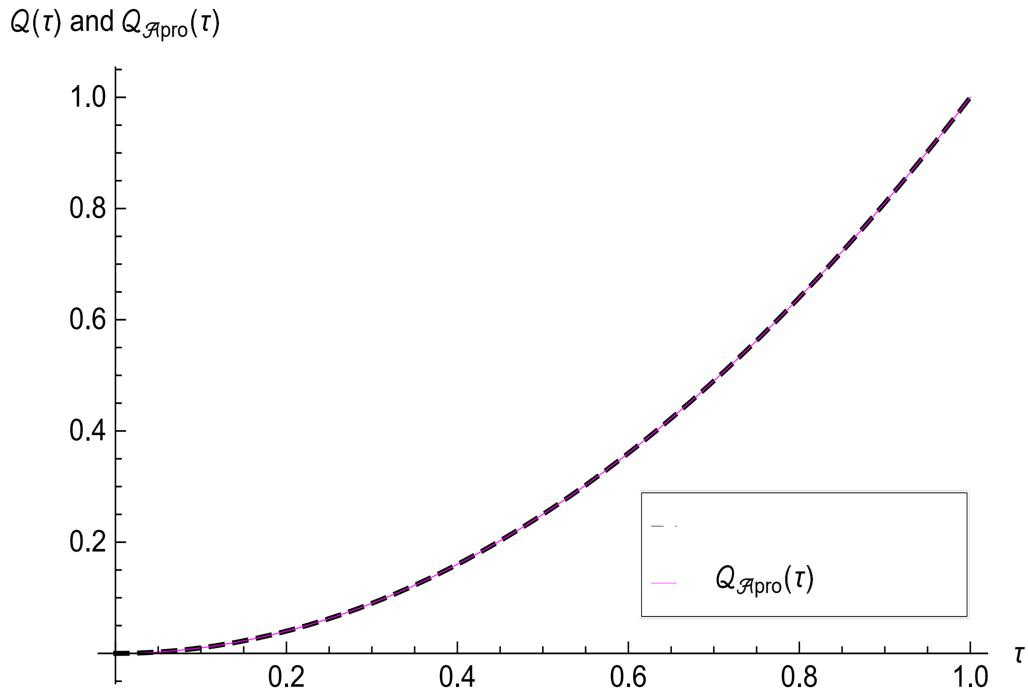

Figure 12. Curves of the exact and numerical solutions of $\mathcal{Q}(\tau)$ of the problem (33), where $\sigma_1 = \varrho_1 = \sigma_2 = \varrho_2 = 0$, $\nu = 0.9$ and $\mathcal{N} = \mathcal{M} = 16$.

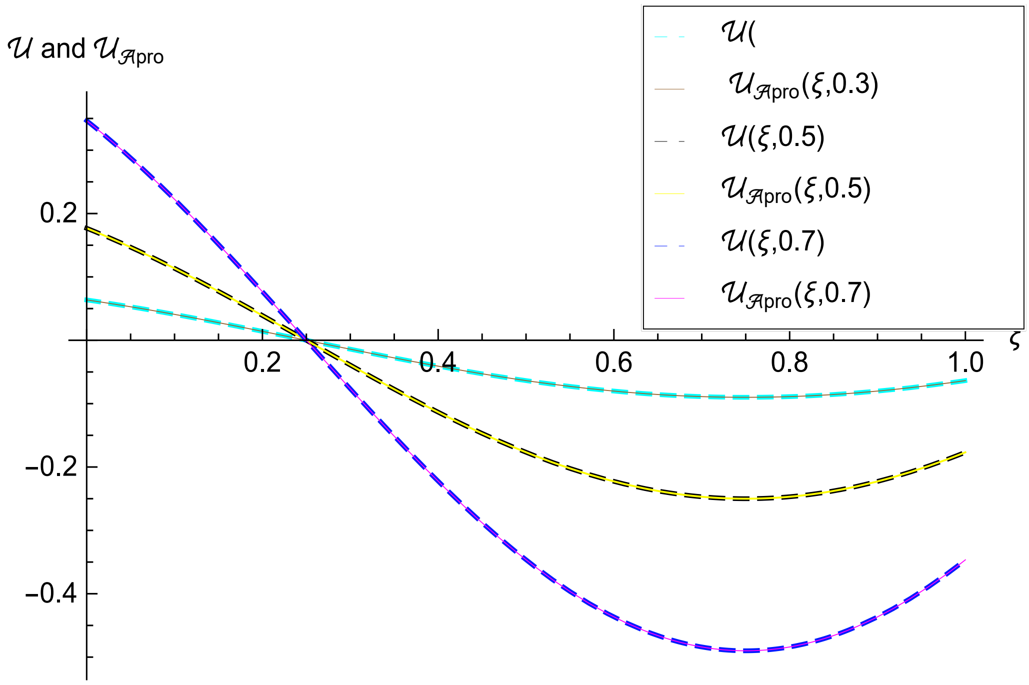

Figure 13. x-Curves of the exact and numerical solutions of $\mathcal{U}(\xi,\tau)$ of the problem (33), where $\sigma_1 = \varrho_1 = \sigma_2 = \varrho_2 = 0$, $\nu = 0.9$ and $\mathcal{N} = \mathcal{M} = 16$.

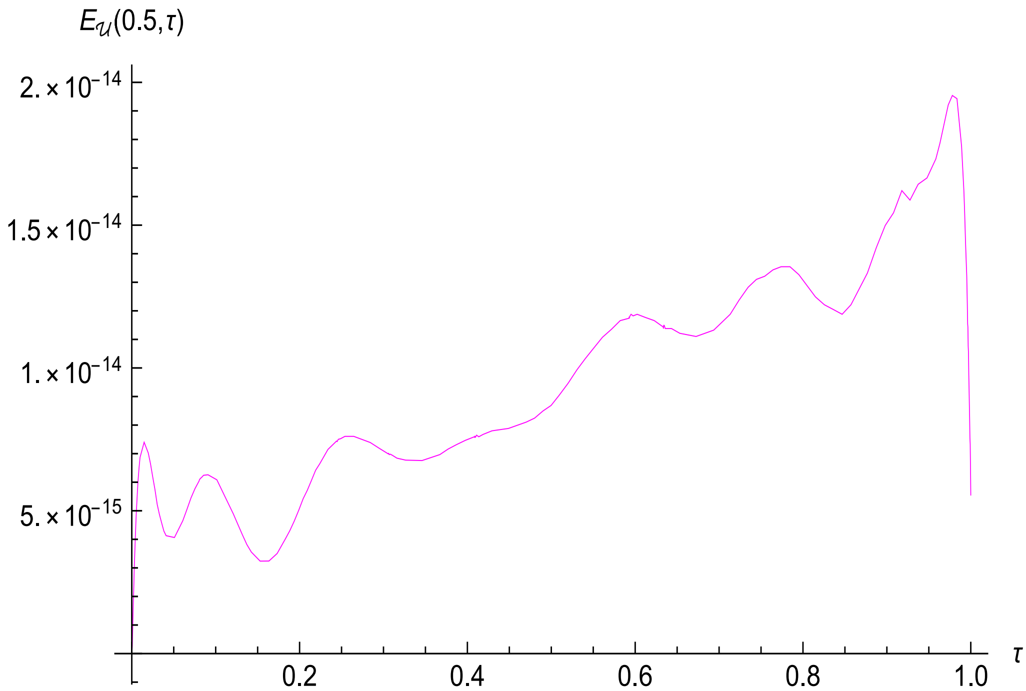

Figure 14. τ-Absolute errors $E_{\mathcal{U}}(0.5,\tau)$ graph of the problem (33), where $\sigma_1 = \varrho_1 = \sigma_2 = \varrho_2 = 0$, $\nu = 0.9$ and $\mathcal{N} = \mathcal{M} = 16$.

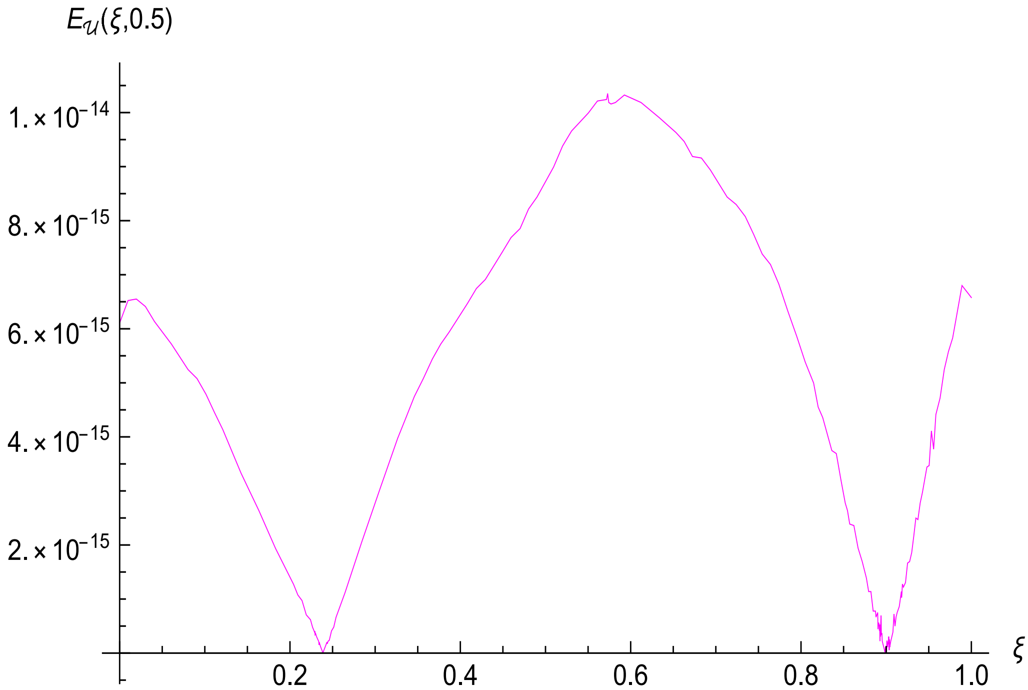

Figure 15. ξ-Absolute errors graph $E_{\mathcal{U}}(\xi, 0.5)$of the problem (33), where $\sigma_1 = \varrho_1 = \sigma_2 = \varrho_2 = 0$, $\nu = 0.9$ and $\mathcal{N} = \mathcal{M} = 16$.

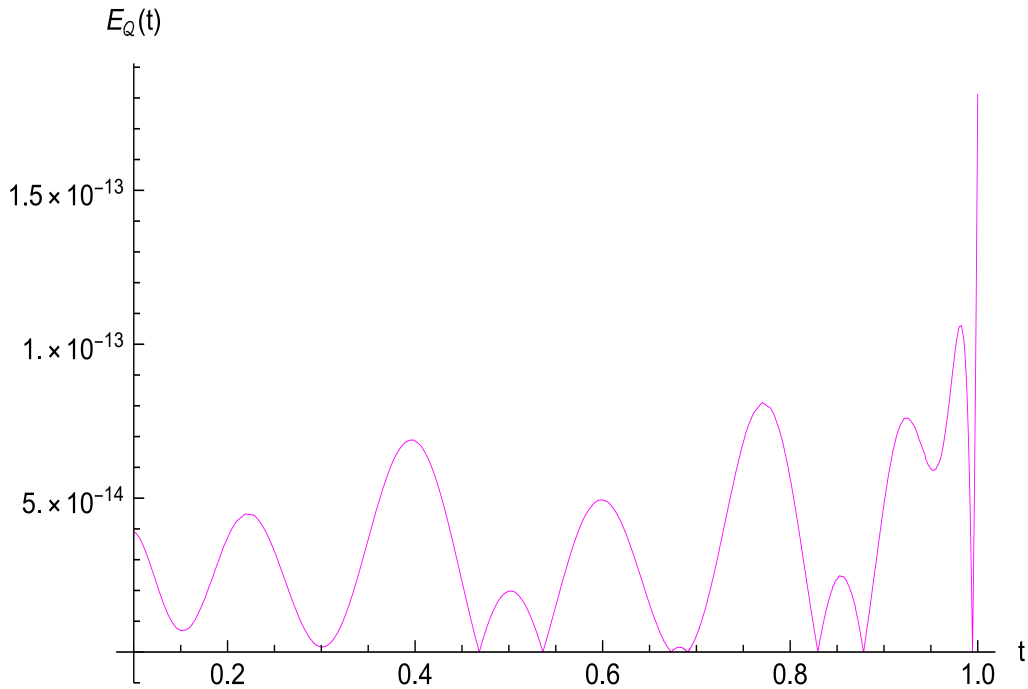

Figure 16. Absolute errors $E_{\mathcal{Q}}(\tau)$ graph of the problem (33), where $\sigma_1 = \varrho_1 = \sigma_2 = \varrho_2 = 0$, $\nu = 0.9$ and $\mathcal{N} = \mathcal{M} = 16$.

5. Conclusions

We have constructed fully shifted Jacobi collocation schemes to study the time-fractional IHEs. Various orthogonal polynomials can be acquired as a particular case of the shifted Jacobi polynomials, such as the shifted Chebyshev of the first or second or third or fourth kind, shifted Legendre, and shifted Gegenbauer. Recently, shifted Jacobi polynomials have been used for solving fractional problems via collocation techniques and have acquired growing popularity due to the ability to obtained the approximate solution depends on the shifted Jacobi parameters σ and ϱ. The powerful proposed approach yielded impressive numerical results that demonstrate the algorithm's great efficiency. The study was treated with both local and nonlocal conditions. The algorithm's results open the way for more studies in this field to be conducted in the future to display additional results in the future.

Author Contributions: Data curation, M.A.A., A.Z.M.A., M.M.B., A.S.A., M.A.Z. and R.M.H.; Formal analysis, M.A.A., A.Z.M.A., M.M.B., A.S.A., M.A.Z. and R.M.H.; Funding acquisition, M.A.A.; Methodology, M.A.A., A.Z.M.A., M.A.Z. and R.M.H.; Software, M.A.A., A.Z.M.A., A.S.A. and M.A.Z.; Writing—original draft, M.A.A., A.Z.M.A., M.M.B., A.S.A., M.A.Z. and R.M.H.; Writing—review and editing, M.A.A., A.Z.M.A., M.A.Z. and R.M.H. All authors contributed equally. All authors have read and agreed to the published version of the manuscript.

Funding: This research was supported by the Deanship of Scientific Research at Imam Mohammad Ibn Saud Islamic University through Research Group no. RG-21-09-05.

Institutional Review Board Statement: Not applicable.

Informed Consent Statement: Not applicable.

Data Availability Statement: Not applicable.

Acknowledgments: The authors extend their appreciation to the Deanship of Scientific Research at Imam Mohammad Ibn Saud Islamic University for funding this work

Conflicts of Interest: The authors declare no conflict of interest.

References

1. Herrmann, R. *Fractional Calculus: An Introduction for Physicists*; World Scientific: Singapore, 2011.
2. Tarasov, V.E. *Fractional Dynamics: Applications of Fractional Calculus to Dynamics of Particles, Fields and Media*; Springer Science & Business Media: Berlin/Heidelberg, Germany, 2011.
3. West, B.J. *Fractional Calculus View of Complexity: Tomorrow's Science*; CRC Press: Boca Raton, FL, USA, 2016.
4. Kilbas, A.A.; Srivastava, H.M.; Trujillo, J.J. *Theory and Applications of Fractional Differential Equations*; Elsevier: Amsterdam, The Netherlands, 2006; Volume 204.
5. West, B.J. *Nature's Patterns and the Fractional Calculus*; De Gruyter: Berlin, Germany, 2017.
6. Seki, K.; Wojcik, M.; Tachiya, M. Fractional reaction-diffusion equation. *J. Chem. Phys.* **2003**, *119*, 2165–2170. [CrossRef]
7. Baleanu, D.; Magin, R.L.; Bhalekar, S.; Daftardar-Gejji, V. Chaos in the fractional order nonlinear Bloch equation with delay. *Commun. Nonlinear Sci. Numer. Simul.* **2015**, *25*, 41–49. [CrossRef]
8. Shen, S.; Liu, F.; Liu, Q.; Anh, V. Numerical simulation of anomalous infiltration in porous media. *Numer. Algorithms* **2015**, *68*, 443–454. [CrossRef]
9. Podlubny, I. *Fractional Differential Equations: An Introduction to Fractional Derivatives, Fractional Differential Equations, to Methods of Their Solution and Some of Their Applications*; Elsevier: Amsterdam, The Netherlands, 1998.
10. Sumelka, W.; Łuczak, B.; Gajewski, T.; Voyiadjis, G. Modelling of AAA in the framework of time-fractional damage hyperelasticity. *Int. J. Solids Struct.* **2020**, *206*, 30–42. [CrossRef]
11. Podlubny, I. *Fractional Differential Equations*; Academic Press: San Diego, CA, USA; Boston, MA, USA, 1999.
12. Zhou, Y.; Zhang, Y. Noether symmetries for fractional generalized Birkhoffian systems in terms of classical and combined Caputo derivatives. *Acta Mech.* **2020**, *231*, 3017–3029. [CrossRef]
13. Eidelman, S.D.; Kochubei, A.N. Cauchy problem for fractional diffusion equations. *J. Differ. Equ.* **2004**, *199*, 211–255. [CrossRef]
14. Luchko, Y. Some uniqueness and existence results for the initial-boundary-value problems for the generalized time-fractional diffusion equation. *Comput. Math. Appl.* **2010**, *59*, 1766–1772. [CrossRef]
15. Metzler, R.; Klafter, J. Boundary value problems for fractional diffusion equations. *Phys. A Stat. Mech. Appl.* **2000**, *278*, 107–125. [CrossRef]
16. Yuste, S.; Acedo, L.; Lindenberg, K. Reaction front in an A + B $\rightarrow$ C reaction-subdiffusion process. *Phys. Rev. E* **2004**, *69*, 036126. [CrossRef] [PubMed]
17. Liu, F.; Burrage, K. Novel techniques in parameter estimation for fractional dynamical models arising from biological systems. *Comput. Math. Appl.* **2011**, *62*, 822–833. [CrossRef]
18. Yu, B.; Jiang, X.; Wang, C. Numerical algorithms to estimate relaxation parameters and Caputo fractional derivative for a fractional thermal wave model in spherical composite medium. *Appl. Math. Comput.* **2016**, *274*, 106–118. [CrossRef]
19. Liu, F.; Anh, V.; Turner, I. Numerical solution of the space fractional Fokker–Planck equation. *J. Comput. Appl. Math.* **2004**, *166*, 209–219. [CrossRef]

20. Metzler, R.; Klafter, J. The random walk's guide to anomalous diffusion: a fractional dynamics approach. *Phys. Rep.* **2000**, *339*, 1–77. [CrossRef]
21. Fan, W.; Jiang, X.; Qi, H. Parameter estimation for the generalized fractional element network Zener model based on the Bayesian method. *Phys. A Stat. Mech. Appl.* **2015**, *427*, 40–49. [CrossRef]
22. Cannon, J.R.; van der Hoek, J. Diffusion subject to the specification of mass. *J. Math. Anal. Appl.* **1986**, *115*, 517–529. [CrossRef]
23. Cannon, J.R.; Esteva, S.P.; Van Der Hoek, J. A Galerkin procedure for the diffusion equation subject to the specification of mass. *SIAM J. Numer. Anal.* **1987**, *24*, 499–515. [CrossRef]
24. Huang, C.H.; Lin, C.Y. Inverse hyperbolic conduction problem in estimating two unknown surface heat fluxes simultaneously. *J. Thermophys. Heat Transf.* **2008**, *22*, 766–774. [CrossRef]
25. Yang, C.y. Direct and inverse solutions of the two-dimensional hyperbolic heat conduction problems. *Appl. Math. Model.* **2009**, *33*, 2907–2918. [CrossRef]
26. Tang, D.; Araki, N. An Inverse Analysis to Estimate Relaxation Parameters and Thermal Diffusivity with a Universal Heat Conduction Equation 1. *Int. J. Thermophys.* **2000**, *21*, 553–561. [CrossRef]
27. Wang, L.; Liu, J. Total variation regularization for a backward time-fractional diffusion problem. *Inverse Probl.* **2013**, *29*, 115013. [CrossRef]
28. Zhang, Y.; Xu, X. Inverse source problem for a fractional diffusion equation. *Inverse Probl.* **2011**, *27*, 035010. [CrossRef]
29. Bhrawy, A.H. An efficient Jacobi pseudospectral approximation for nonlinear complex generalized Zakharov system. *Appl. Math. Comput.* **2014**, *247*, 30–46. [CrossRef]
30. Bhrawy, A.H. A Jacobi spectral collocation method for solving multi-dimensional nonlinear fractional sub-diffusion equations. *Numer. Algorithms* **2016**, *73*, 91–113. [CrossRef]
31. Bhrawy, A.H.; Abdelkawy, M.A.; Baleanu, D.; Amin, A.Z. A spectral technique for solving two-dimensional fractional integral equations with weakly singular kernel. *Hacet. J. Math. Stat.* **2018**, *47*, 553–566. [CrossRef]
32. Abdelkawy, M.A.; Doha, E.H.; Bhrawy, A.H.; Amin, A.Z. Efficient pseudospectral scheme for 3D integral equations. *Proc. Rom. Acad. Ser. A Math. Phys. Tech. Sci. Inf. Sci* **2017**, *18*, 199–206.
33. Ameen, I.G.; Zaky, M.A.; Doha, E.H. Singularity preserving spectral collocation method for nonlinear systems of fractional differential equations with the right-sided Caputo fractional derivative. *J. Comput. Appl. Math.* **2021**, *392*, 113468. [CrossRef]
34. Abdelkawy, M.A.; Amin, A.Z.; Bhrawy, A.H.; Machado, J.A.T.; Lopes, A.M. Jacobi collocation approximation for solving multi-dimensional Volterra integral equations. *Int. J. Nonlinear Sci. Numer. Simul.* **2017**, *18*, 411–425. [CrossRef]
35. Doha, E.; Abdelkawy, M.; Amin, A.; Baleanu, D. Spectral technique for solving variable-order fractional Volterra integro-differential equations. *Numer. Methods Partial. Differ. Equ.* **2018**, *34*, 1659–1677. [CrossRef]
36. Doha, E.H.; Bhrawy, A.H.; Abdelkawy, M.A.; Van Gorder, R.A. Jacobi–Gauss–Lobatto collocation method for the numerical solution of 1+ 1 nonlinear Schrödinger equations. *J. Comput. Phys.* **2014**, *261*, 244–255. [CrossRef]
37. Doha, E.H.; Abdelkawy, M.A.; Amin, A.Z.; Baleanu, D. Approximate solutions for solving nonlinear variable-order fractional Riccati differential equations. *Nonlinear Anal. Model. Control.* **2019**, *24*, 176–188. [CrossRef]
38. Bhrawy, A.H.; Zaky, M.A.; Baleanu, D. New numerical approximations for space-time fractional Burgers' equations via a Legendre spectral-collocation method. *Rom. Rep. Phys.* **2015**, *67*, 340–349.
39. Bhrawy, A.H.; Zaky, M.A. Highly accurate numerical schemes for multi-dimensional space variable-order fractional Schrödinger equations. *Comput. Math. Appl.* **2017**, *73*, 1100–1117. [CrossRef]
40. Bhrawy, A.; Zaky, M. An improved collocation method for multi-dimensional space–time variable-order fractional Schrödinger equations. *Appl. Numer. Math.* **2017**, *111*, 197–218. [CrossRef]
41. Bhrawy, A.; Doha, E.; Baleanu, D.; Ezz-Eldien, S.; Abdelkawy, M. An accurate numerical technique for solving fractional optimal control problems. *Differ. Equ.* **2015**, *15*, 23.
42. Bhrawy, A.H.; Abdelkawy, M.A. A fully spectral collocation approximation for multi-dimensional fractional Schrödinger equations. *J. Comput. Phys.* **2015**, *294*, 462–483. [CrossRef]
43. Abdelkawy, M.; Zaky, M.A.; Bhrawy, A.H.; Baleanu, D. Numerical simulation of time variable fractional order mobile-immobile advection-dispersion model. *Rom. Rep. Phys.* **2015**, *67*, 773–791.
44. Hendy, A.S.; Zaky, M.A.; Hafez, R.M.; De Staelen, R.H. The impact of memory effect on space fractional strong quantum couplers with tunable decay behavior and its numerical simulation. *Sci. Rep.* **2021**, *11*, 1–15. [CrossRef]
45. Diethelm, K.; Ford, N.J. Analysis of fractional differential equations. *J. Math. Anal. Appl.* **2002**, *265*, 229–248. [CrossRef]